NTNU – Trondheim
Norwegian University of
Science and Technology

Effect of Copper Content on etching Response of Aluminum in Alkaline and Acid Solutions

Morten Dahlstrøm

Materials Technology
Submission date: June 2012
Supervisor: Otto Lunder, IMTE
Co-supervisor: Kemal Nisancioglu, IMT

Norwegian University of Science and Technology
Department of Materials Science and Engineering

I hereby declare that this work has been performed individually and in accordance to the regulations for master projects at the Norwegian University of Science and Technology (NTNU).

Trondheim, June 2012

Morten Dahlstrøm

Preface

This work was carried out at the Norwegian University of Science and Technology (NTNU) in the period 15/01/2012 to 15/06/2012.

First of all, I would like to thank my supervisor Otto Lunder[1] and Kemal Nisancioglu[2] for their assistance and guidance trough out my master project. Furthermore, David Franke[3] kindly helped med and showed med around in the corrosion laboratory, and Kjell Røkke[4] helped me with the equipment that I needed for my work.

[1] SINTEF
[2] NTNU
[3] Ph.D student at NTNU
[4] Division engineer at Corrosion laboratory

Sammendrag

Kobber blir brukt som et legeringselement i aluminium legeringer for å øke deres mekaniske styrke. Ved å blande kobber med aluminium vil den ellers så gode korrosjonsmotstanden til rent aluminuim bli svekket og legeringen vil få en lavere motstand mot korrosjon. Etter år med forskning på korrosjon i aluminium legeringer har flere resultater vist en økende korrosjonsrate hos aluminium som har blitt legert med både sink og kobber. Disse legeringselementene forårsaker et fenomen kalt ”grainy appearance”. Ved å blande kobber i aluminium har også korngrensekorrosjon blitt oppdaget etter varmebehandling av legeringen.

Før legeringene i dette prosjektet ble etset i surt og alkalisk miljø ble legeringene undersøkt med Glow Discharge Mass Spectroscopy (GDMS) for å kunne konstantere korrekte mengder av legeringselementer og urenheter i legeringene. Etseforsøk har blitt utført på rent aluminium (Al 5N), aluminium tilsatt 10 ppm kobber (AlCu10), aluminium tilsatt 100 ppm kobber (AlCu100) og aluminium tilsatt 1000 ppm kobber (AlCu1000). Korrosjonspotensial tester har også blitt gjort av disse legeringene. Videre har også overflaten av alle legeringer som har blitt utsatt for etseforsøk blitt undersøkt i lysmikroskop, Scanning Electron Microscopy (SEM), Electron Backscattered Diffraction (EBSD), Confocal Microscope (IFM), Energy Dispersive Spectroscopy (EDS) og Glow Discharge Optical Electron Spectroscopy (GD-OES). Disse metodene har blitt brukt for å måle høydeforskjeller mellom etsede nabokorn, bestemme krystallstrukturen til etsede korn, måle overflateruheten til etsede korn, detektere hvilke elementer som finnes i overflaten til etsede prøver og for å gi en dybdeprofil av de etsede prøvene.

I de alkaliske etseprøvene ble det funnet at et økende kobberinnhold i aluminiumslegeringen gav en økt korrosjonsrate. Men AlCu10 legeringen viste liten eller ingen forskjell fra den rene legeringen, dette gjaldt også i korrosjonspotensial testene. Ved å øke kobberinnholdet økte også korrosjonspotensialet dramatisk for AlCu100 og AlCu1000 legeringene. Videre ble også en økt etsehastighet oppdaget for korn som hadde krystallografisk orientering nær [111] planet etter alkalisk etsing, en forskjell i overflateruheten ble også målt mellom korn med forskjellige krystallografiske orienteringer etter alkalisk etsing. GD-OES undersøkelser av prøver som hadde blitt etset i alkalisk miljø viste en forskjell i dybdeprofilen etter hvilke temperatur de ble etset på og hvordan de ble behandlet etter etsing. AlCu1000 legeringen ble også undersøkt etter å ha blitt utsatt for sure etseforsøk i HCl syre. Denne legeringen viste en annen respons til etsebadet og en annen overflate etter etsing enn hva den gjorde etter alkalisk etsing.

Summary

Copper are used as an alloying element in aluminum alloys to increase the strength of the material. By mixing copper and aluminum the good corrosion resistance of the pure aluminum decreases giving the alloy a lower corrosion resistance. After years of investigation on corrosion of aluminum alloys several results have shown increasing corrosion rates of aluminum that have been alloyed with both copper and zinc, giving a “grainy appearance” on the surface of the alloy. By adding copper to the aluminum increased intergranular corrosion and preferential etching of surface grains has been found after heat treatment and etching of the alloy.

Before etching the aluminum alloys in alkaline and acidic environments, Glow Discharge Mass Spectroscopy (GDMS) measurements was done for all the alloys to determine the correct amount of alloying elements and impurities in each alloy. Preliminary etching trials have been performed on pure aluminum (Al 5N), aluminum containing 10 ppm copper (AlCu10), aluminum containing 100 ppm copper (AlCu100), and aluminum containing 1000 ppm copper (AlCu1000), as well as corrosion potential tests. Further, the surface of all the etched test specimens has been investigated in light microscope, Scanning Electron Microscope (SEM), Electron Backscattered Diffraction (EBSD), Confocal Microscope (IFM), Energy Dispersive Spectroscopy (EDS),and Glow Discharge Optical Electron Spectroscopy (GD-OES). These methods have been used to determine height differences between etched neighboring grains, the crystallographic orientation of grains, surface roughness, detecting elements occurring on the surface of etched specimens, and giving a depth profile of the etched specimens.

For the alkaline etching trials, an increasing etching rate was found by increasing the amount of copper in the alloys, however the AlCu10-alloy showed little or no difference from the pure aluminum both in the etching trials and the corrosion potential tests. By increasing the copper amount in the aluminum the corrosion potential increased drastically for AlCu100-alloy and the AlCu1000-alloy. Further an increasing etching rate of grains having close to [111] crystallographic orientation could be seen in alkaline environment, a difference in the surface roughness between grains with different crystallographic orientations could also be seen for the alkaline etched test specimens. The GD-OES investigations done on test specimens that had been alkaline etched revealed differences in their depth profiles dependent on the etching temperature and how the specimens was treated after being etched. AlCu1000-alloys etched in acidic environment showed a different type of etching and surface after etching than the other alloys etched in the same environment. A clear difference could also be seen between the alkaline and the acidic etched AlCu1000 specimens.

Table of Contents

CHAPTER 1

Introduction

Due to the increasing use of aluminum and its alloys for both architectural and structural purposes, lots of work has been done the last years to understand corrosion of aluminum. Normally aluminum is looked at as a material with high corrosion resistance and low mechanical properties. To increase the mechanical properties it is normal to use alloying elements such as Mg, and Si, and in some cases Cu, Mn and Cr. Extrusion and rolling of aluminum is a widely used methods to create structures such as pipes, bumpers for cars, sheets for decoration, and other structures. Normally these structural elements are etched and anodized after the extrusion to give a better surface look, and to increase the corrosion resistance. In other aluminum products such as parts used in planes and space applications high strength are needed and copper are used as an alloying element. By using copper as an alloying element the corrosion resistance of the aluminum decreases dramatically even at small amounts.

The Norwegian aluminum producer Hydro has had problems with rolled aluminum plates getting an uneven surface look after being etched and anodized. This phenomenon is called “grainy appearance” or “streaking” and is a result of some grains etching more than others. This problem has been investigated for a long time without being fully understood, but it has been tracked back to issues in the production process. Research has mainly been done working with Zn as the main alloying element causing these unwanted etching results. Results show that grains having a crystallographic orientation close to [111] show a higher etching rate in alkaline environments compared to the [110] and the [100].

Results from research done on etching of aluminum and zinc have also shown traces of copper on the surface of the etched aluminum and from discussions it has been proposed that this element also might having something to do with the preferential etching of aluminum alloys. This project will therefore concentrate on aluminum alloyed with small amounts of copper to see how this affects the corrosion resistance in both alkaline and acidic environments. Intergranular corrosion will also be investigated. By producing aluminum-copper alloys from pure materials this project will attempt to isolate the etching problem so that little or no trace elements from other particles will affect the results. The alloys will be tested in weight loss experiments (alkaline and acidic), the corrosion potential will be measured, the crystallographic orientation of grains will be determined as well as the surface roughness and height differences between neighboring grains. All this will be done to see how the copper affects the corrosion of aluminum alloyed with copper.

CHAPTER 2

Literature review

2.1 Alkaline etch

Sodium hydroxide (NaOH) is the most used alkaline etching media for etching aluminum and it can be used with or without additives.

When etching aluminum using NaOH hydrogen is produced as a bi product of the aluminate production that only appears in alkaline solutions. The etching ability of the alkaline NaOH solution decreases as the aluminum etching goes on over time due to an increasing aluminum content in the solution and due to the hydrogen development that removes the hydrogen from the NaOH. This only becomes a problem in highly worked industrial size etching baths and should not be a problem in smaller laboratory tests. Due to the chemical reactions happening in the etching bath during etching, the corrosion rate is slowing down in highly worked etching baths due to a lower electrically conductivity and a higher viscosity {1}.

One problem that can occur during alkaline etching using NaOH as an etching media is a sudden tendency for pitting on the surface of the test specimen. Due to the high corrosion rate at a small area during pitting, local higher temperature can speed up the etching rate by as much as 300% at the pitting points, causing an uneven etching of the surface. As seen in figure 2.1 the corrosion rate of aluminum increases drastically with an increasing temperature in the etching media and by etching aluminum alloyed with copper the etching rate would probably be even higher due to the galvanic difference between aluminum and copper. By etching aluminum alloys in NaOH energy will be released creating an exothermic reaction that affects the temperature of the etching bath and controlling the temperature is therefore an important aspect of the alkaline etching process {2}. Controlling the temperature of the etching media can be done by lowering the etching bath into a water bath controlled by a thermostat keeping the temperature constant trough out the entire etching time.

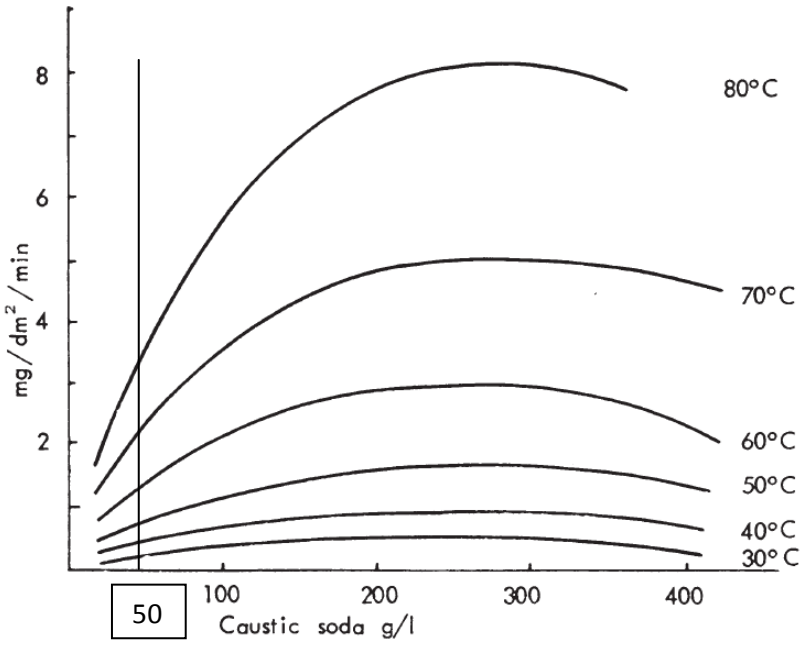

Figure 2.1: Graph showing etching rate of pure aluminum in different concentrations of NaOH at different temperatures. Vertical line indicates the amount of NaOH used in this project.

Preferential etching of grains on the aluminum surfaces is a problem that has been investigated by the industry for some time now. When etching extruded and rolled aluminum surfaces in an alkaline environment before anodizing, the grain structure on the surface can appear uneven something that is unwanted when producing aluminum that is supposed to have an even surface look. Earlier research on this subject has been looking at zinc as the main alloying element causing these preferential etching problems on aluminum surfaces. By dissolving small amounts of zinc into the alkaline etching bath, tests have reveled preferential grain etching or, so called “grainy appearance” on extruded test specimens of AlMgSi(Zn) aluminum alloy that had been tempered and artificially aged to T6 strength{3}. Results from etching trials on these test alloys showed that an increasing amounts of zinc in the test samples gave an increased surface roughness value on test specimens that had been alkaline etched after been polished. From corrosion tests there was also found that with an increasing amount of Zn in the alloy an increasing susceptibility to preferential grain etching was found. After EBSD analyzes it was concluded that the grains that had etched the most had orientation [111], while the least etched grains had a near [001] orientation, a clear correlation between the etching topography and the surface concentration of Zn also was seen. Near the surface of the deeper etched grains there was discovered a higher amount of Zn and Cu than on the less etched grains {4}. If the Zn on the surface was depleted on to the surface from the Zn added to the bath or diffused from the bulk material, or both, is not known. Weight loss tests done on aluminum with dissolved Zn in the etching bath showed a lower weight loss with an increased zinc level and a stabilization of the weight loss was observed at 20 ppm Zn added {5}.

Research done on neighboring grains with crystallographic surface planes [334], [225], and [119] on pure aluminum, by Koroleva et. al.{6}. Showed that by rounding off to the nearest low index plane there was found that the largest height difference after etching existed between grains showing surface orientation close to the [001] and the [111] crystallographic orientation. By measuring the

open circuit potential of the two different grains there was also found a drop of 20 mV from the less etched [001] to the most etched grain [111] {7}.

When etching aluminum containing copper a smut layer forms on the surface of the test specimen after a few minutes of etching. If height differences or roughness are going to be measured on the test sample it is important to remove this smut layer before the investigations. Too remove this unwanted layer it is possible to clean the test specimen using 65% nitric acid at 25^{o}C since this acid does not attack aluminum. There is also a possibility to use a mixture of chromic and phosphoric acid, called Chromium Phosphoric acid. The composition normally used are 7wt% phosphoric acid and 4 wt% chromic acid between 90-100^{o}C. This mixture rapidly dissolves any smut layer formed on aluminum without affecting the aluminum alloy as long as no heavy metals are present in the solution {8}.

2.2 Acid etch

Normally from alkaline etching of aluminum and aluminum alloys there have been found a higher etching rate on grains with [111] crystallographic orientation on the surface, without this phenomena being fully understood. It has been proposed that it might have something to do with the higher surface tension in the [111] orientation compared to the other crystallographic orientations. Investigation of corrosion behavior on 99,999% pure aluminum has also been done using acidic etching baths containing hydrochloric acid (HCl) as an etching media. This research found that by using four different concentrations of HCl acid that the etching response of the pure aluminum changed with the changing HCl concentrations. The paper {9} also proposed that the etching rate of the different crystallographic orientations was different in HCl compared to alkaline etching. Results from the research can be seen in table 2.2 where the type of corrosion and the etching rate of the different crystallographic orientations are shown for the different concentrations of HCl.

Table 2.2: Table showing acidic etching results for pure aluminum etched in acidic environments. Normally the [111] orientation shows the highest etching rate when etching pure aluminum in alkaline environments, but from the table it can be seen that the [110] oriented grains showed a higher etching rate in acidic environment {9}.

HCl aq. Solution	Low ⟷ High Corrosion sensitivity	Local Corrosion
11,6 mol/L	{100} {111} {110}	Pits
5,8 mol/L	{111} {100} {110}	Intergranular
2,9 mol/L	{111} {100} {110}	Pitting (little)
1,5 mol/L	{111} {100} {110}	Pitting (much)

From table 2.2 it is possible to see that the [110] crystallographic orientation has the highest sensitivity to corrosion regardless of the acid concentration. This result is quite different from the etching results shown when etching aluminum in alkaline environment where the [111] orientation normally has the highest etching rate.

2.3 Selective dissolution

Alloys produced from two or more alloying elements that has a difference in the standard potential, has shown the alloy characteristic shown in figure 2.3.a where the less noble material (A) corrodes away faster than the more noble material (B) in the alloy. The features shown in figure 2.3.a are not possible to measure with an ammeter due to the reactions happening during dissolution in the alloy. Some of the reasons for this is the hydrogen development on the surface and the passivity occurring during dissolution is so strong that it prevents an active region. Region (a) in figure 2.3.a is a low current region where the current is produced due to dissolution of the less noble (A) material and the etching of (A) is suppressed by a layer of the more noble metal (b) that forms on the surface, it is not completely clear if the surface layer produced during dissolution is a pure B layer or a B-enriched layer. There have been found differences between dissolution in cold worked and annealed samples where the cold worked samples shows a much higher dissolution rate of (A) compared to the annealed samples. But after about 1 hour of higher etching rate the rate falls to the same level as for the annealed sample. A reason for this mechanism is that defects occurring during cold working of metals such as point, line, and planar defect that increases the diffusion rate for the alloy. Another proposed mechanism is that the metal layer forms by nucleation and growth of pure B crystals via surface diffusion. There have also been discussed if the surface mobility decreases with increasing potential and content of the less noble metal. E_C is a proposed potential where the surface is unstable and a pitting-type of attack occurs. This potential is the point where transition from (a) to (b) occurs and an increasing dissolution of (A) increases sharply with the increasing corrosion potential. The dissolution that happens in (a) and (b) increases as the ΔE^{o} of the alloy system increases, this also means that an increasing amount of B in the system decreases the tendency of (a) and (b) dissolution {10}.

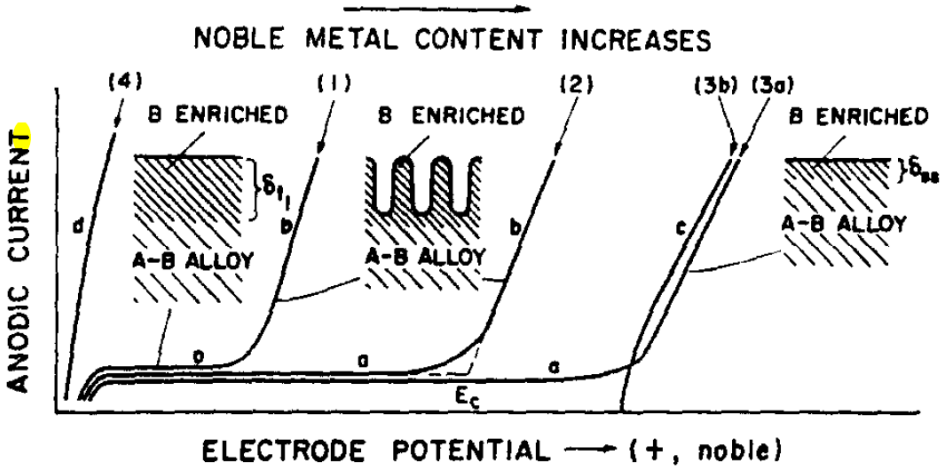

Figure 2.3.a: An illustration showing the anodic polarization behavior of binary A-B alloys. Curves (1), (2), and (3a) are due to dissolution of A, and curve (3b) to dissolution of B. δ_{t1} and δ_{t2} are the diffusion layer thicknesses at time 1 and steady state. {10}

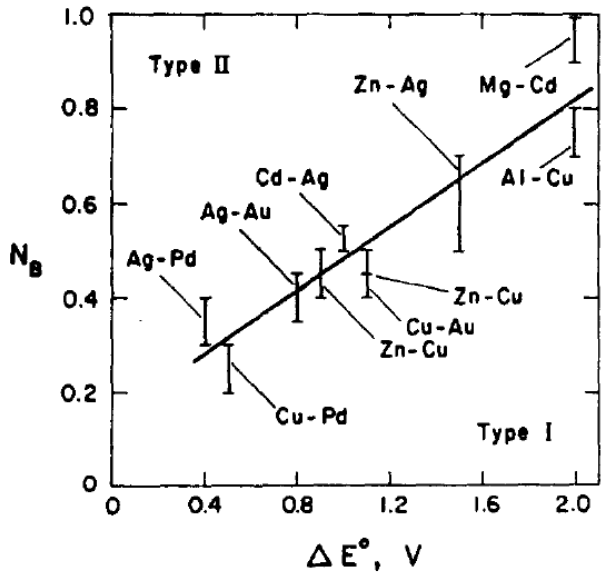

Figure 2.3.b: A plot that illustrates that the mole fraction N_n of the more noble material B for transition from (a), (b) to (c) dissolution increases as the difference in standard reduction potential of the metals in the alloy increases (E_B°-E_A°) {10}.

From figure 2.3.b it can be seen that 0,7-0,9 mole fraction of Copper in Aluminum gives an ΔE° of 2V in the transition from (a)-(b) dissolution to (c). N_B is the composition at which the transition between de-alloying which occurs in region (b) and non-selective dissolution which occurs in region (c). From figure 2.3.a it can be seen that region (b) shows a pitting-type of attack resulting in a porous surface compared to the even distribution of B on the surface in (a). At region (a)-(c), dissolution occurs when the content of B in the alloy is at the level where the potential needed for dissolving B occurs {10}.

Significant amounts of copper have been found on the surface of Al 2024-T3 that has been mechanically and chemically polished in a mixture of concentrated sulfuric, phosphoric, and nitric acids. The surface enrichment of copper was here believed to result from de-alloying of intermetallic S-phase particles (Al_2CuMg) which was found to account for about 60% of the particles on the alloy surface. Investigations showed that de-alloying resulted in nano-porous Cu-rich remains that resulted in pitting around the periphery of the particles. After exposing the Al 2024-T3 alloy to 0.1 molar NaOH or 0.5 molar NaCl solution a significant enrichment of elemental Cu was found on the surface {11}.

Due to oxygen reduction around copper rich particles on the surface of aluminum alloys, the particles might work as cathodes and thereby provoke corrosion of the aluminum matrix around the Cu-particles. Further corrosion and dealloying of the S-phase (Al_2CuMg) due to preferential dissolution of aluminum, produces a copper-rich, nano-porous layer on the surface. Selective dissolution of Al-Cu alloys may also lead to formation of metallic copper on the surface of the alloy {12}. In the first stage of corrosion of aluminum-copper alloys, only the aluminum oxidizes while the oxide film grows. During this stage, copper enriches in a thin layer beneath the growing oxide film, close to the bulk/oxide border. And after a certain amount of copper has been enriched in this layer, the copper starts to oxidize at the same rate as it is accumulated from the bulk material keeping the copper layer at a constant thickness. The copper and aluminum ions migrate into the oxide film proportionally to their concentration in the bulk material of the alloy. Copper moves faster than aluminum in an

aluminum-copper alloy and therefore the main film will be depleted in copper relative to the copper amount in the bulk alloy. Due to etching of the aluminum around the copper particles, the copper are usually lost to the solution when they reach the film surface, but a layer of copper-rich oxide may still form at the surface of the film. When etching aluminum alloys in an alkaline environment an oxide layer of 1-5 nm might for at the alloy/film interface and dissolve at the same rate at the oxide/solution interface. Copper might also be reduced or lost to the etching bath from flaws in the film surface where copper particles forms {13}.

2.4 Intergranular corrosion (IGC)

Intergranular Corrosion (IGC) on heat treated aluminum alloys containing copper is not an unusual phenomena {14}. Due to coppers high diffusion rate during heat treatment of aluminum-copper alloys it segregates towards the grain boundaries forming galvanic paths around the grains causing galvanic corrosion of the grain boundaries. By investigating aluminum alloy AA6xxx, AlMgSi containing copper. There has been found that alloys with 0.02 wt% copper were not susceptible to IGC in an alkaline environment, using NaCl as an etching media. When increasing the Cu content to 0,18 wt %, the alloy showed corrosion when it was in the naturally aged T4 condition, and by underaging the alloy it showed highly susceptibility to IGC on the entire test surface {15}.

For aluminum alloys containing a low amount of copper (0.004 %), artificial aging towards the T6 peak strength have given the alloy a decreased susceptibility to IGC. As for aluminum alloys containing a higher amount of Cu (0.18 %) no big differences was show in the corrosion susceptibility after underaging for 42 minutes, and peak aging for 24 hours, while water quenched alloys has shown high susceptibility in the T4 temper {16}. Svenningsen et al {17} showed that the heat treatment was of a significant importance to the IGC resistance of a extruded AA6xxx alloy containing (wt %) 0.5Mg, 0.6Si, 0.2Fe, 0.2Mn, and about 0.02 to 0.2 wt% Cu. In Svenningsen's research there was also seen that alloys with low Cu content did not show signs of IGC.

2.5 Crystal structure in aluminum

Aluminum has the face-centered cubic (FCC) crystal structure shown in figure 2.5 where there is one atom in each corner of the cube, and one on each side, figure 2.5 also shows the three different crystallographic planes appearing in the FCC structure. From investigation of the different planes it can be found that the [111] plane has both a higher packing factor (table 2.5), meaning how tight the atoms are packed in the crystallographic plane, and a higher surface tension than the other planes. This is something that might be affecting the corrosion rate of the [111] planes compared to the [001] and [101] planes. By using Electron backscattered Diffraction (EBSD) it is possible to find the crystallographic orientation of each grain appearing in the surface of a metal.

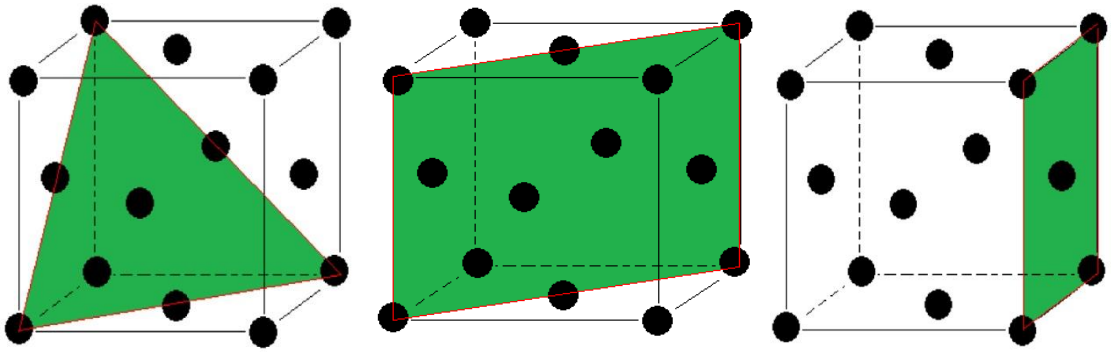

Figure 2.5: Figure showing the three main crystallographic planes occurring in the aluminum FCC structure. From left: [111], [101], and [001].

Table 2.5: Table showing the packing factors for the three crystallographic planes shown in figure 2.5.

Plane	Packing factor
[111]	0,91
[101]	0.56
[001]	0,79

2.6 Aluminum-copper alloy

Aluminum is classed as a reactive and easily oxidized element. But in real life it shows a high resistance to corrosion both as a pure metal and when alloyed with manganese and magnesium. The reason for the high corrosion resistance is due to the thin, compact, and firmly adherent oxide film that forms on the surface of aluminum. Corrosion on aluminum generally only happens when an oxide solvent media comes in contact with the surface dissolving the surface layer before attacking the metal. Aluminum does not have high mechanical strength in its pure metal form, therefore copper are added to the alloy to increase the mechanical strength of the material, this also decreases the corrosion resistance of the aluminum alloy drastically. As little as 0.1 atm. % copper in the aluminum alloy drastically increases the corrosion rate {18}.

When alloying light weight metal such as aluminum it is important to get an even distribution of the alloying elements so that the material properties become homogenous throughout the entire specimen. Aluminum has a lower density and a lower melting point compared to copper, and if the copper are not added in the right way to the melt, the aluminum alloy can suffer an uneven copper distribution. To avoid this problem it is normal to use a master-alloy[5] {19}, a master alloy is also preferential to use when small amounts of alloying material are to be used. Due to the more equal distribution of the alloying element that this method gives, and because of the higher accuracy of the alloying element that can be achieved, this is a preferred method to use when alloying aluminum with small amounts of heavier materials.

2.7 Aluminum copper phases

From figure 2.7 it can be seen that the solubility of copper in aluminum is 5.7 atm % at the eutectic temperature (548.2^{o}C), and at 250^{o}C this solubility sinks to between 0.1 and 0.2 atm % {20}.

Between 0.2 and 5.7 atm % Cu, two equilibrium solid states can appear. Above the solidus curve in figure 2.7, the copper is 100% soluble, and when the temperature is held above this temperature for a longer period of time, this permits the needed diffusion for the copper to go into solid solution. At temperatures below this solidus line, the equilibrium state consists of solid solution, α, and an intermetallic compound phase, θ (Al_2Cu).
By rapid cooling of a supersaturated solid solution (SSS) aluminum-copper system, a sequence off precipitates is developed. These precipitates develop either with increasing temperature or with increasing time at temperature between room and the temperature at the solidus line. The sequence off the precipitates developing is showed in the following notation {21}:

$$SSS \rightarrow GP\ zones \rightarrow \theta'' \rightarrow \theta' \rightarrow \theta\ (Al_2Cu)$$

By naturally aging the aluminum-copper alloy in the range between -20^{o}C to 60^{o}C disc like planar aggregates, Guinier-Preston zones (GP-zones), forms from the randomly distributed copper atoms parallel to the [001] plane in the α aluminum {22}. These zones form strain fields that again increases the alloys resistance to deformation due to increasing elastic coherency stress that forms internally hardening. At higher temperatures Al_2Cu forms and increases the strength even further {23}.

[5] Alloy with a higher content of the wanted alloying element.

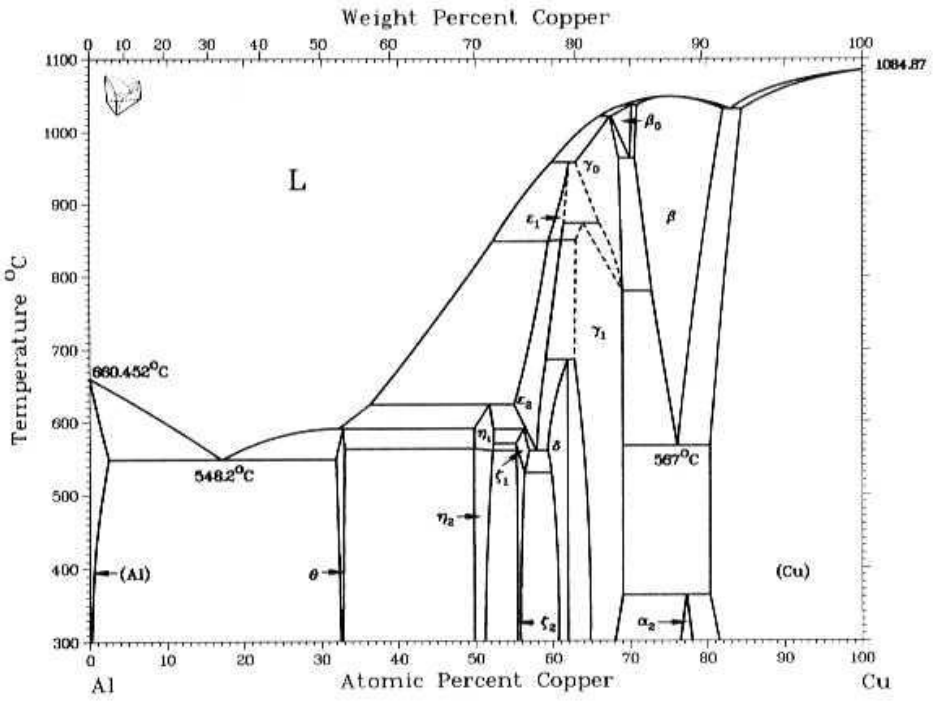

Figure 2.7: Figure showing phase diagram for aluminum copper.

2.8 Experimental techniques

2.8.1 Electron Backscattered Diffraction (EBSD)

By using Electron Backscattered Diffraction (EBSD) in a Scanning Electron Microscopy (SEM) it is possible to determine the crystallographic orientation on the surface of grains in metallic materials. By placing a test specimen in the SEM chamber and then tilting the sample up to 70° compared to the electron beam as illustrated in figure 2.8.1.a, a higher amount of backscattered electrons are created so that as many backscattered electrons as possible hits the phosphor screen on the detector creating signals for the Kikuchi bonds. The electrons that are reflected back from the test specimen (backscattered electrons) within the Bragg's angle will create "Kikuchi lines" that forms a Kikuchi pattern (figure 2.8.1.b) on a phosphor screen in the detector. The lines created in the Kikuchi pattern represent the crystallographic plane on the surface of the metal specimen. And as the electron beam moves around the test specimen, the crystallographic orientation changes when the beam crosses the border from one grain to another. By using known maps it is possible to find the crystallographic orientation from the pattern created by the backscattered electrons {24}. By using EBSD it is possible to investigate the crystallographic orientation of etched specimens to see if there are any differences in the crystallographic orientation between highly etched grains, and less etched grains.

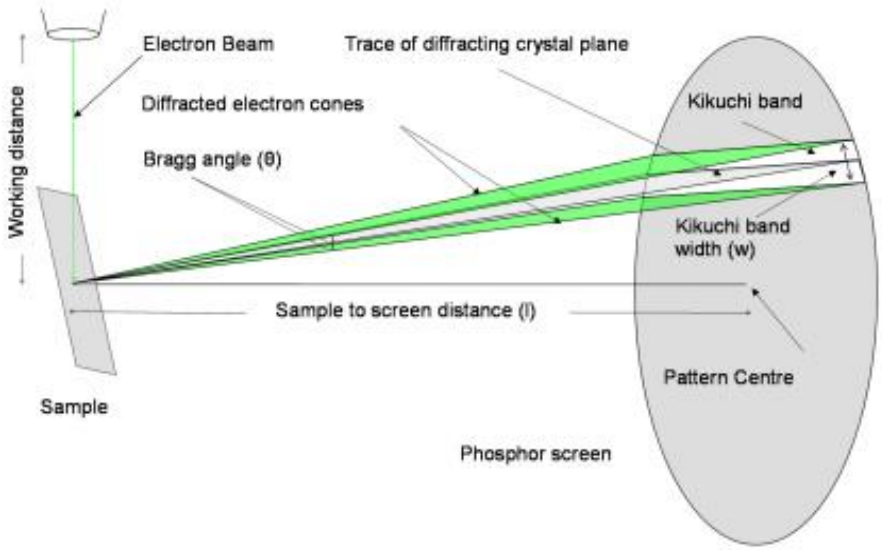

Figure 2.8.1 a: Figure showing EBSD-setup inside the SEM. Electrons hits the test specimens and secondary electrons get reflected onto the phosphor screen, creating Kikuchi bands which represents the crystallographic orientations {25}.

By indexing the results created in the SEM, color maps showing the crystallographic orientation of each grain on the metal surface can be created. Figure 4.1.2.a is an example of a color map created by EBSD. By comparing the color of each grain to the Inverse Pole Figure shown in figure 4.1.2.b the crystallographic orientation of each grain can be decided.

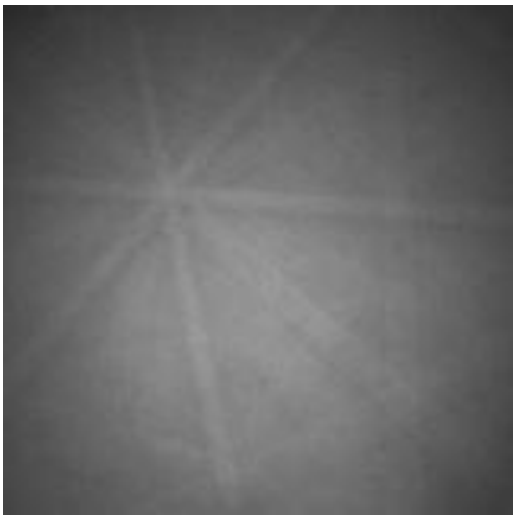

Figure 2.8.1 b: Picture showing Kikuchi lines in an aluminum sample containing 1000 ppm copper.

2.8.2 Glow Discharge Optical Emission Spectroscopy (GD-OES)

Glow Discharge Optical Emission Spectrometry (GD-OES) uses sputtering and atomic emission to provide a depth profile of materials. Figure 2.8.2 shows the mechanism of the GD-OES.

By applying vacuum to the chamber in front of the test specimen, the specimen is hold in place and a surface area is exposed to the vacuum chamber. Two separated surfaces inside the vacuum chamber form a cathode and an anode. When voltage is applied between these two surfaces, the argon gas in the chamber becomes ionized. The argon ions bombard the cathode surface causing sputtering of the test specimen. The sputtered atoms diffuse into the negative glow region where they are excited

and emit elemental characteristic optical emission, due to the homogeneous electric field a flat bottom crater is obtained on the test specimen. By analyzing the signals created from the excited atoms, it is possible to decide what type of material that has been emitted and a depth profile can be made of the test specimen showing type of material, depth of material layers, and the amount of each material {25}.

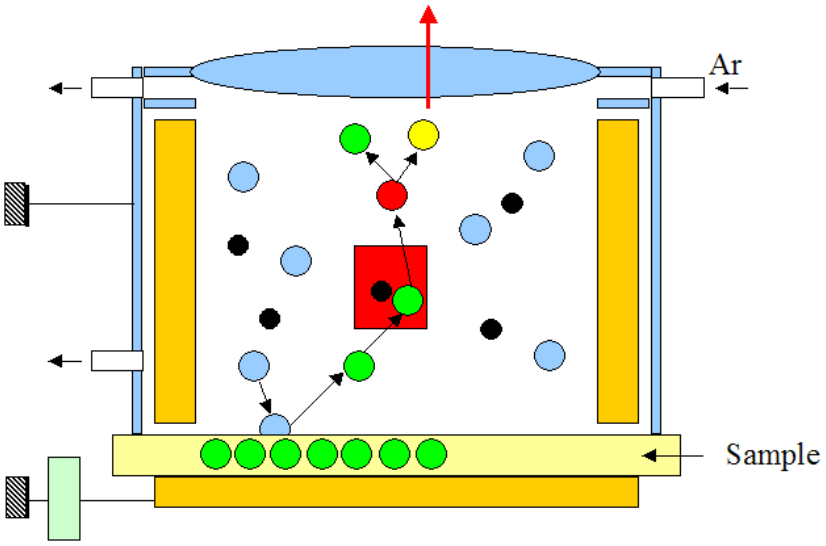

Figure 2.8.2: Figure showing how the vacuum chamber in the GD-OES works {25}.

2.8.3 Energy Dispersive Spectroscopy (EDS)

By using EDS detection in a SEM it is possible to investigate type and amount of the particles occurring on the surface, and some distance into the test specimen, depending on the acceleration voltage being used. By bombarding the test specimen with primary electrons it is possible to detect the X-rays being emitted when a primary electron strikes an electron in the K-shell of an atom. When an atom is exited like this an electron from the L-shell jumps into the vacancy in the K-shell, creating X-rays with the same energy as the energy difference between the two shells. These x-rays are then used to determine the type of element that have been exited, the amount of x-rays are used to determine the amount of each phase that occurs in the volume tested.

2.8.4 Confocal Microscope (IFM)

By using Confocal Microscopy (IFM) it is possible to create a 3-dimensional picture of the surface investigated. This is done by selecting a surface to investigate and then decide for two focusing points, one point below the specimen surface, and one above the specimen surface. The microscope then takes pictures with a given distance, between these two focusing points. The pictures are then put on top of each other to create a 3-dimentional image of the surface. Figure 2.8.4 shows an example of a typical 3-D image created by IFM microscopy. By using special software it is possible to find both the roughness and the height differences on the investigated surface.

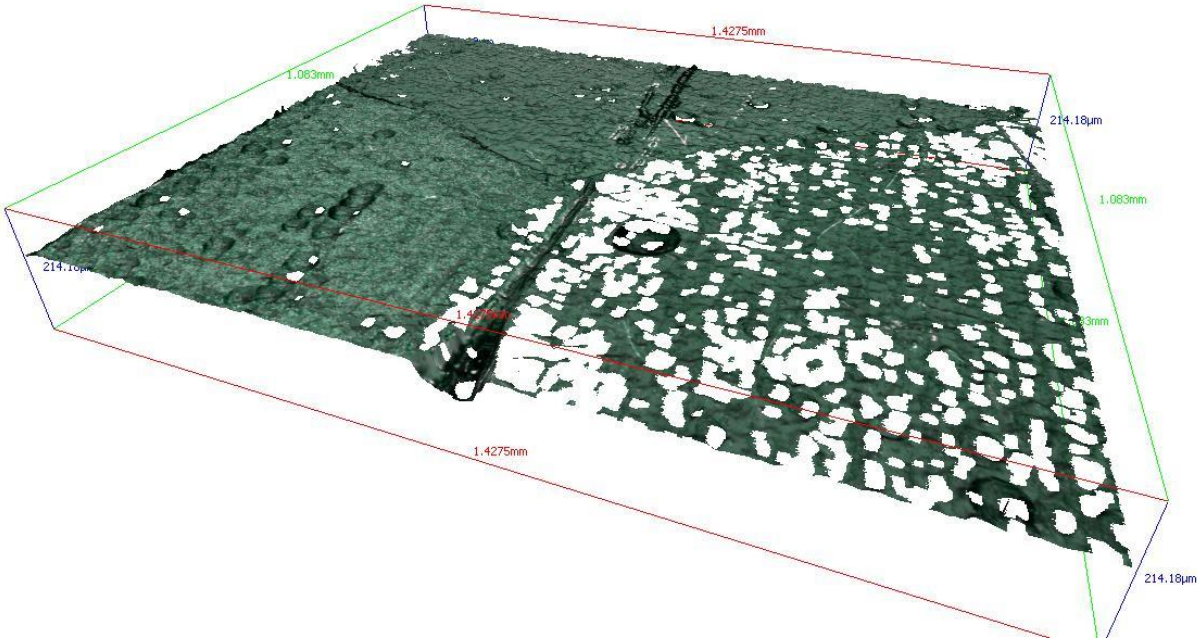

Figure 2.8.4: Figure showing a 3-dimentional picture used to measure roughness and height differences between surface grains on a aluminum surface.

CHAPTER 3

Experimental

3.1 Materials

The type of aluminum-copper alloy used in this project was decided on the background of how copper affects aluminum in alkaline environment. Pure aluminum was produced to have a reference alloy while the 10, 100, and 1000 ppm alloys was produced to see how small amounts of copper affected the aluminum compared to larger amounts (1000 ppm).

To get an even distribution of copper in the aluminum melt a master alloy was made. When producing alloys containing smaller amounts of alloying elements, using a master alloy gives a better distribution of the alloying elements in the finished alloy. The master alloy is also important to avoid that the heavier material sinks to the bottom of the furnace, creating an uneven melt.
To create a master alloy for this project pure aluminum and pure copper was melted together creating an alloy containing approximately 2 wt % copper. After production the master alloy was measured by weight and mixed with the correct amount of pure aluminum to give the desired Al-Cu alloys decided to be used in this project. After doing a bulk analysis using Glow Discharge Mass Spectroscopy (GDMS) a more correct result for the amount of alloying elements was given. GDMS uses a gas discharge or plasma atomization/ ionization source to ionize atoms in the alloy. By measuring the wavelength of the energy released from electrons moving from one shell to another the type of element and the amount of each element can be found with high accuracy. Table 3.1 shows the different elements and the amount (weight ppm) in each alloy. The reason for the relatively high amount of copper in the pure aluminum is due to impurities from the dies used to produce the aluminum bars.

Table 3.1: Table showing alloying elements and trace elements found by GDMS measurements in the four different alloys produced for this project. Numbers in weight ppm.

Alloy	Si	Fe	Cu	Zn	Pb
Al 5N	0,9±0,1	1,6±0,0	3,0±0,2	0,6±0,2	0,7±0,2
AlCu 10	3,2±1,1	0,6±0,3	10,6±2,4	0,6±0,3	0,7±0,3
AlCu 100	1,0±0,1	0,5±0,0	78,4±6,0	0,4±0,1	0,3±0,1
AlCu 1000	2,9±1,6	0,5±0,0	619,4±49,0	0,3±0,2	0,4±0,1

The pure aluminum and master alloy was melted together in an electric furnace at 750^{o}C for approximately 1.5 hours, poured into a die, and air cooled at room temperature. After cooling the surfaces of the aluminum bar's was milled off to remove slag and impurities created under melting and cooling, and to create smooth surfaces ideal for rolling. From the approximately 2x2x5 cm casted

and milled aluminum bars, strips approximately 2mm thick and 5 cm wide where cold rolled and cut into desired test size pieces. For both the alkaline and the acidic etching trials the rolled alloys where heat treated in an electric furnace at 600^{o}C for one hour before being rapidly cooled in cold water. This step was done to create a more even grain structure and to relieve internal stress created during rolling.

3.2 Etching trials

3.2.1 Alkaline etch

For the alkaline etching trials strips of approximately 5x2 cm were cut and a hole was drilled in each specimen for attachment of fishing line during etching trials (figure 3.2.1, right). The surfaces of the test specimens were then grinded with 1000 SiC grinding paper to ensure an even surface finish on all the test specimens. A 1.25 molar NaOH (50g/litre) solution was used as an etching media. The NaOH was mixed with distilled water and stirred with a magnetic stirrer, each etching trial used 3 dl NaOH solution for each test specimen. The etching trials were carried out at two different temperatures, 25^{o}C, and 70^{0}C where the 25^{o}C test was carried out over 60 minutes while the 70^{o}C test was carried out over 10 minutes due to the increase in reactivity between the aluminum alloy and the etching media at increasing temperatures, this can be seen in Figure 2.1. Before each etching trial the test specimens was cleaned with acetone and ethanol, and dried with a heating gun before being weighed.

The setup for the etching trials can be seen in the left picture of figure 3.2.1 showing the etching bath lowered into a water tank hold at a constant temperature by a thermostat. The test specimens where hung into the etching bath using fishing line that was attached to a glass pipe as seen in figure 3.2.1. After each etching trial the test specimens was gently cleaned in distilled water, rinsed in 65 % nitric acid, and again gently cleaned in distilled water to remove any nitric acid.

Figure 3.2.1: Left picture showing etching setup. Right picture showing test specimen used for etching trials after being grinded with 1000 SiC paper.

3.2.2 Acid etch

For the acid etch trials a solution of 4 molar hydrochloric acid (HCl) was mixed from. 12 molar hydrochloric acid fuming 37% that was mixed into distilled water and stirred with a magnetic stirrer. Each etching trial was carried out using 200 ml etching baths lowered into a water bath kept constant at 25^{o}C by a thermostat. The acid etching trials was carried out on the same test specimens that had been used in the alkaline trials so that the results from the investigations of the surface after each etching test could be compared.

Before each etching trial the test specimens were mechanically grinded with 1000 SiC paper and cleaned with acetone and ethanol before being dried with a heating gun and then weighed. The etching trial was carried out in the same way as for the alkaline etching (figure 3.2.1). Due to the low etching rate of AlCu alloys at 25^{o}C in HCl in the first few hours of each test, the alloy containing 1000ppm copper was the only alloy tested. Each test trial was carried out until the specimen showed extreme hydrogen development (after ca. 5 hours), then they where let to etch for 15 minutes before being taken out of the etching bath. After each etching trial the specimens was lowered into distilled water to remove the HCl acid, rinsed in 65 % nitric acid before again being gently cleaned in distilled water.

3.3 Corrosion potential

For the corrosion potential trials the test specimens was pretreated in the same way as for the alkaline and the acid etching trials, no holes was drilled in these test specimens. Further an area on each specimen was covered in tape before being coated with Miccroshield as seen in figure 3.3.a, 1µm polished surface and 1000 SiC grinded surfaces was tested to see how the coating responded to the different surface roughness. After a quick etching trial the coating showed best adhesion to the 1000 SiC grinded surface so this surface finish was used trough out the corrosion potential trials. Figure 3.3.a shows test specimen before being used in corrosion potential test.

Figure 3.3.a: Picture shows test specimen after being coated with Miccroshield.

Corrosion potential tests were carried out on all aluminum alloys used in this project at both 25^{o}C and 70^{o}C. The 25^{o}C tests were carried out over 90 minutes while the 70^{o}C tests were carried out over 10 minutes due to the high etching rate at this temperature. The higher temperature also decreased the lifetime of the coating causing it to dethatch from the surface after about 10 minutes. Each test was carried out in an etching bath containing 300 ml of 1.25 molar NaOH solution (same as for the

etching trials). The container holding the etching media was lowered into a water bath to keep the temperature constant trough out the entire test period. The salt bridge used was made by mixing 5.6 gram of KOH with 100 ml distilled water that was heated to approximately 75^{o}C before 10-12 grams of Agar was added. For the reference bath a 2 molar mixture of KOH was used with a XR400 Hg/HgO reference electrode from radiometer Analytical. Before each etching trial the specimens was cleaned with ethanol and dried with a heating gun.

When lowering the test sample into the etching bath it is important that the sample is placed vertical so that the hydrogen developed during etching flows away from the surface and not becoming trapped creating a "protective surface layer" against the NaOH solution. For measuring the corrosion potential the setup showed in figure 3.3.b was used. To log the corrosion potential a 34970A Data Acquisition/ Switch unit from Hewlett Packard was used together with Agilent Bench Link Data Logger 3 software.

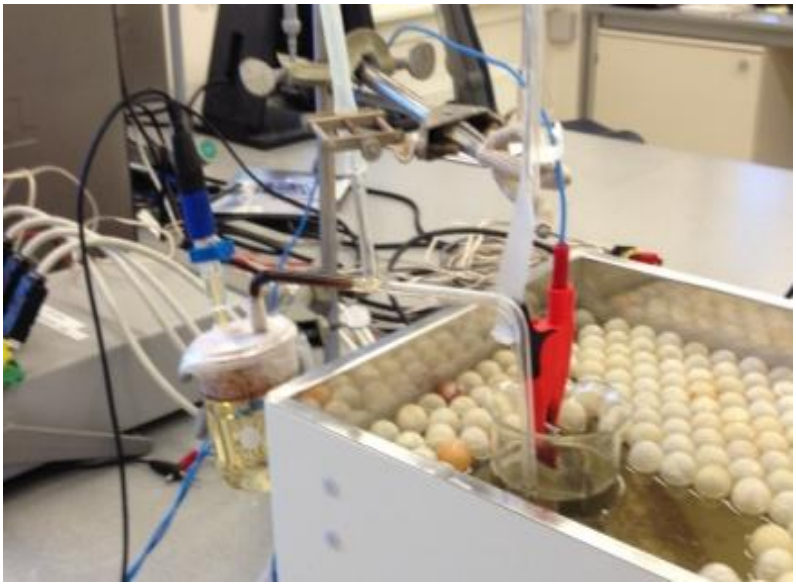

Figure 3.3.b: Picture showing the setup for the corrosion potential tests. The salt bridge connects the reference bath containing the reference electrode with the etching bath. The test sample is connected to the logger unit with a clamp creating a circuit with the reference bat and the etching bath.

As for the corrosion potential testing in acidic environment the same setup as described for the alkaline trials was used. Each etching bath contained 300 ml solution of 4 molar HCl acid at 25^{o}C. Due to the low boiling point of HCl, 25^{o}C tests were the only one carried out.

3.4 Intergranular corrosion (IGC)

Test specimens used to investigate intergranular corrosion (IGC) was produced from the alloys containing copper. This was done by heat treating the alloys at 600^{o}C for one hour before the oven was switched off, and the alloys were let to cool down inside the oven for 22 hours until they reached room temperature. Each test specimen was then grinded using 1000 SiC paper to create an even surface before being cleaned in acetone and ethanol, and dried with a heating gun. Etching was carried out at 25^{o}C for one hour in the same 1.25 molar NaOH solution used for the other etching trials. After etching the test specimen was gently cleaned in distilled water, nitrite acid, and distilled water. The setup of the etching trial was the same as described in chapter 3.2.1 and shown in figure 3.2.1.

3.5 Surface characterization

3.5.1 Light microscopy/macroscopy

By using an Axiovert 25 light microscope and a Wild Photomakroskop M 400 macro-scope, etched test specimens was investigated to find neighboring grains that had been etching at different rate creating so called “grainy appearance.” Areas showing height differences between neighboring grains were chosen for further investigation. The same areas selected for investigation after the alkaline etching was also investigated after the sour etching trials to see if different results could be detected.

3.5.2 Electron Backscattered Diffraction (EBSD)

The Electron Backscattered Diffraction (EBSD) analysis was performed using a Zeiss Ultra 55, Limited Edition SEM with an offline EBSD system. Areas found by using light microscopy and macroscopy was analyzed using EBSD to see if there were any differences between the crystallographic orientations on the surface of differently etched neighboring grains. The samples were inserted into the SEM, and tilted 70^{o} compared to the primary electron beam before analyzing. Parameters used during EBSD were:

- Acceleration voltage: 20 kV
- Working distance: 20 mm
- Step size: 0,5-1 µm

After performing the EBSD analysis an offline computer with Nordif software was used to index the results. The rest of the parameters used during the EBSD investigations can be viewed in appendix C.

3.5.3 Energy Dispersive Spectroscopy (EDS)

Energy Dispersive Spectroscopy (EDS) tests have been done on surfaces etched in both alkaline and acidic environments to find the types of elements that was present at the surface and in the first few µm of the test specimen, EDS tests were carried out using the same SEM microscope as used for EBSD investigations. The X-rays produced by the test was processed using Espite EDS indexing software that gives a map of the different elements exited in the tested area. Parameters used of the EDS detection were:

- Acceleration voltage: 13-15 kV
- Working distance. 10mm

3.5.4 Roughness measurements

Grains investigated with EBSD and EDS were further investigated in a Confocal Microscope to see if any differences in the roughness of the different etched grains could be detected, and to measure the height difference between them. The microscope used was an Alicona Infinite Focus capable of creating 3D images of the surface. An IFM microscope is an optical 3D microscope that uses the short depth of focus of an optical light microscope to create a 3D image of the specimen surface. This is done by taking images of a desired amount of focusing planes between two chosen focusing planes. These pictures are then processed by a computer and put on top of each other creating a 3D image of the surface. By investigating these 3D images with Infinite Focusing software from Alicona it is possible to find the surface roughness as well as the height difference between neighboring grains. The Confocal Microscope was also used to look for signs of IGC. By looking for grain boundaries that had been etching more than the grains and measuring the height difference between the grain boundary and the grains IGC could be measured. By using this type of microscope to measure height differences on the surface it is possible to get a higher accuracy on the results compared to measuring height differences using a light microscope. How the roughness is calculated can be viewed in appendix B.

3.5.5 Glow Discharge Optical Emission Spectroscopy (GD-OES)

For the Glow Discharge Optical Emission Spectroscopy (GD-OES) tests the alloys where first wrapped in aluminum foil and heated to 600^{o}C for one hour before they were quenched in water. The surface of each test specimen was then grinded and polished down to a mirror like surface look using; 1000 Sic paper, 2400 Sic paper, 4000 Sic paper, and finally polished down to a 1µm mirror like finish. Each test specimen was then etched with a 1.25 molar NaOH solution for one hour at 70^{o}C and for 6 hours at 25^{o}C before being cleaned with acetone and ethanol. After etching all the test specimens was gently cleaned in distilled water before they were dried with a heating gun. One sample from each test alloy was also desmutted using 65% nitrite acid after being gently cleaned in distilled water before they were lowered into distilled water again, and then dried with a heating gun.GD-OES was used to detect the amounts of different elements in the test specimens as well as how deep into the specimens they occurred, and the thickness of the element layers. The tests were done on all the four different alloys and were done from the surface and 7.5-8 µm into the test specimen. This investigation gave the thickness of oxide layers, and where in the test specimens the different elements occurred as well as the amount of each of the element occurring in the different alloys. The GD-OES tests were carried out at Hydro in Haugesund. Parameters used during investigations can be viewed in appendix D.

CHAPTER 4

Results

4.1 Alkaline etching

4.1.1 Etch rate

Etching experiments done on pure aluminum, and aluminum containing 10, 100 and 1000 ppm copper showed a substantial difference in etching rate. The pure aluminum showed a low rate of etching after being etched for 1 hour at 25^{o}C in 1.25 M NaOH but few signs of preferential etching could be seen, indicating an even etch of the entire surface. During etching only small amounts of hydrogen development on the surface was seen something that also indicates a low etching rate. After weighing the etched pure aluminum only a small loss of mass could be found. For the test alloys with increasing amounts of copper the etching rate increased. The test specimens containing 1000 ppm copper (AlCu1000) showed a high hydrogen development during the entire test period compared to the pure aluminum. Results from the entire test can be seen in figure 4.1.1.a that shows the average etching rate and the variance per minutes for each alloy. When increasing the temperature of the etching bath to 70^{o}C a remarkable increase in the etching rate could be seen, even for the pure aluminum samples. The hydrogen development at the surface of each test specimen could easily be detected after about one second, something that indicated that the etching bath used about one seconds to make the oxide layer protecting the substrate material thin enough for the bulk material to corrode. After about 10-20 minutes of testing higher hydrogen development at some parts of the surface could be seen, indicating that some grains etched faster than others. After weighing each test sample that had been etched a remarkable difference in the etching rate was found between the different alloys, the average etching rate per minute can be seen in figure 4.1.1.b. By comparing the two graphs showing the average etching rate per minute for the two different temperatures the influence of the higher temperature can clearly be seen. After etching AlCu10-alloy in NaOH and cleaning it using nitric acid orange/ rust colored areas on the surface was found by using light microscope. Orange areas formed on the surface of alkaline etched AlCu-alloys that have been cleaned in nitric acid are probably Al_2Cu particles since these particles normally appear as rusty in light microscopy images after exposing aluminum-copper alloys to nitric acid {27}. Figure 4.1.1.c shows an image of the AlCu10 surface.

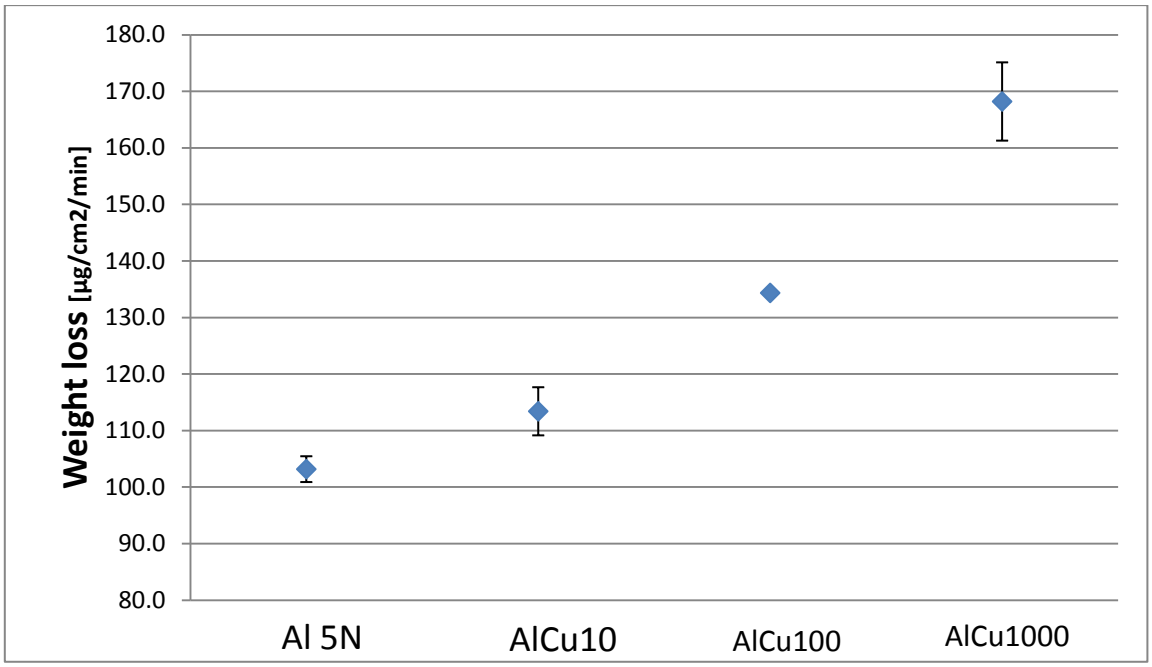

Figure 4.1.1.b: Graph showing the average µg removed from one cm^2 of each test specimen every minute throughout the weight loss test done at 25°C.

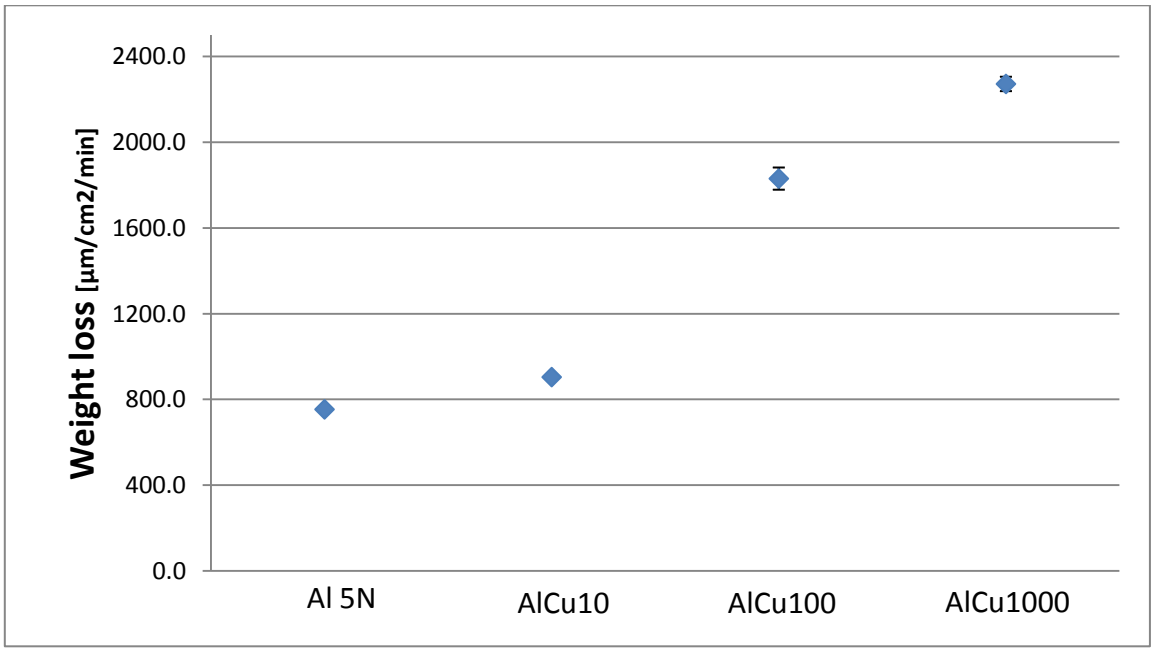

Figure 4.1.1.c: Graph showing the average µg removed from one cm^2 of each test specimen every minute throughout the weight loss test done at 70°C.

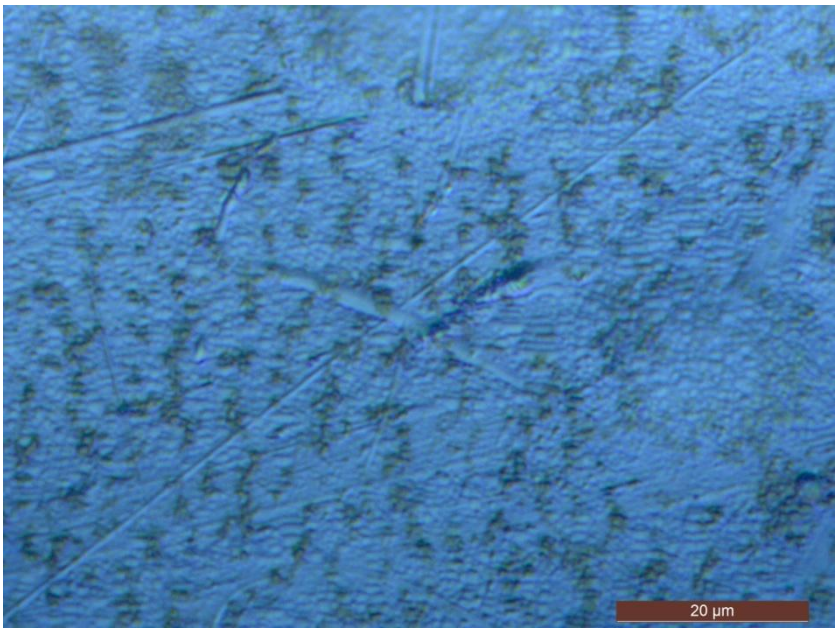

Figure 4.1.1.a: Image showing the surface of an AlCu10-alloy after etching in NaOH and desmutting using nitric acid. Orange/rusty colored areas can be seen indicating Al_2Cu particles that have formed on the surface.

4.1.2 Electron Backscatter Diffraction (EBSD)

Electron Backscattered Diffraction (EBSD) tests was done on test specimens etched in NaOH at 70°C since these samples showed the highest etching rate and the largest height difference between neighboring grains. The EBSD results showed that there was a clear difference of the corrosion rate between grains that had different crystallographic orientations. A higher etching rate could be seen on pure aluminum grains that had a clear [111] orientation and on aluminum-copper grains showing near [111] orientations. Grains close to the [111] crystallographic orientation showed a higher etching rate than the grains having [001] and [101] orientation, results from these tests can be seen in figure 4.1.2a-d. Figure 4.1.2.a shows a representative figure of etched grains on the surface of a pure aluminum sample that have been etched at 70°C for 10 minutes and a clear height difference can be seen between the neighboring grains. The most etched grain (light blue) lies close to the [111] orientation while the two other grains lies closer to the [001] crystallographic orientation, this can be seen by looking at the reverse polarization figure and the plotted reverse polarization figure in figure 4.1.2.b.

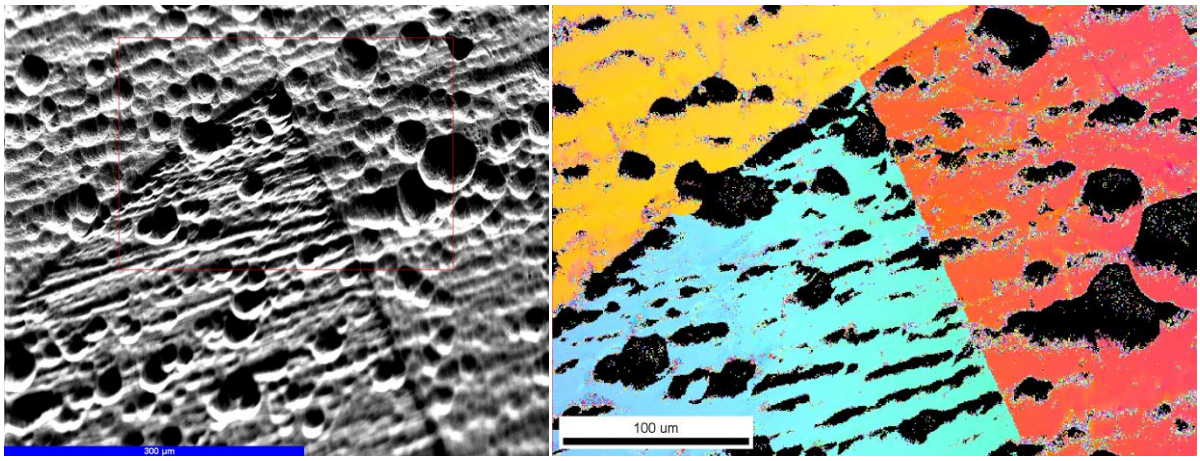

Figure 4.1.2.a: Figure showing three neighboring grains on the surface of a pure aluminum sample that has been etched at 70°C for 10 minutes. It can clearly be seen that the grain close to the [111] (blue) crystallographic orientation has been etched more than the grains closer to the [001] orientation.

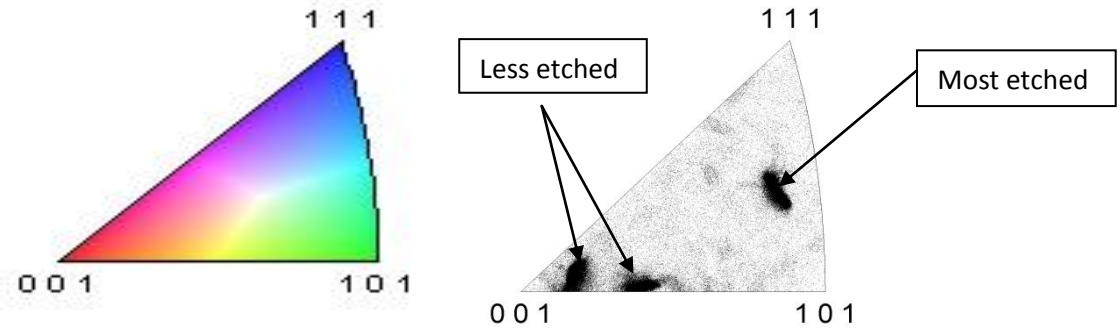

Figure 4.1.2.b: Figure showing the reverse polarization figure (left) being used to determine which types of crystallographic orientations the different grains have. The figure to the right shows where most of the tested points inside each grain ended during the EBSD analysis.

EBSD analysis done on AlCu1000-alloys also showed the same results as the pure aluminum where grains that had been etched more than others had a crystallographic orientation close to the [111] orientation. From the reverse pole figure in figure 4.1.2.d it can be seen that grain 2 and 3 in figure 4.1.2.c are both close to the [111] orientation and has almost the same crystallographic orientation, while the less etched grain (1) has an orientation closer to the [001] orientation. After doing 12 EBSD analyses of AlCu1000-alloys figure 4.1.2.c shows a representative picture on which crystallographic orientations that etches the most. From figure 4.1.2.c it can be seen that grain (1) show less etching than grain (2) and (3).

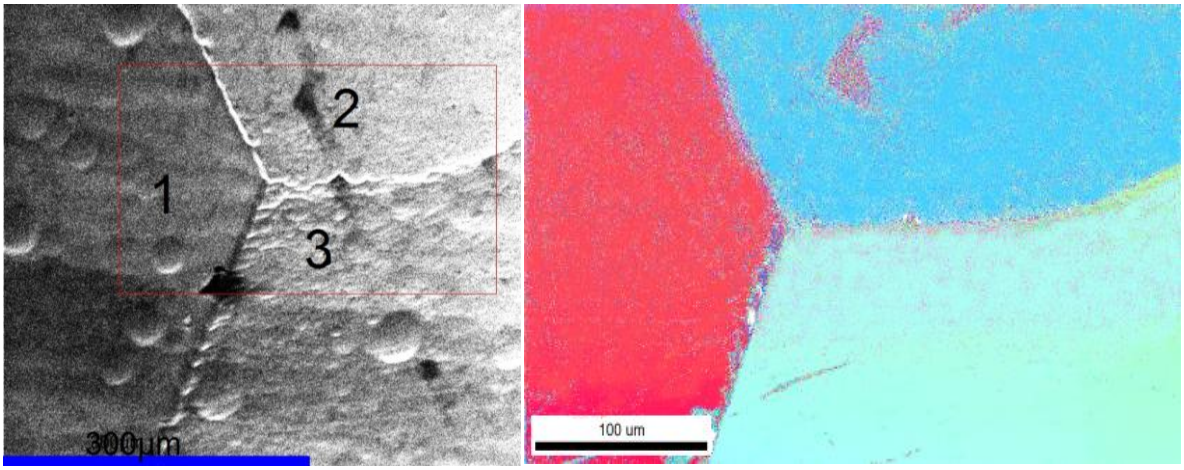

Figure 4.1.2.c: Figure showing an area on an AlCu1000-alloy that has been etched at 70°C for 10 minutes. The left picture shows a SEM picture of the surface clearly showing the height difference between the neighboring grains. The right picture shows a EBSD picture of the three grains giving a clear indication of the crystallographic orientation of each grain.

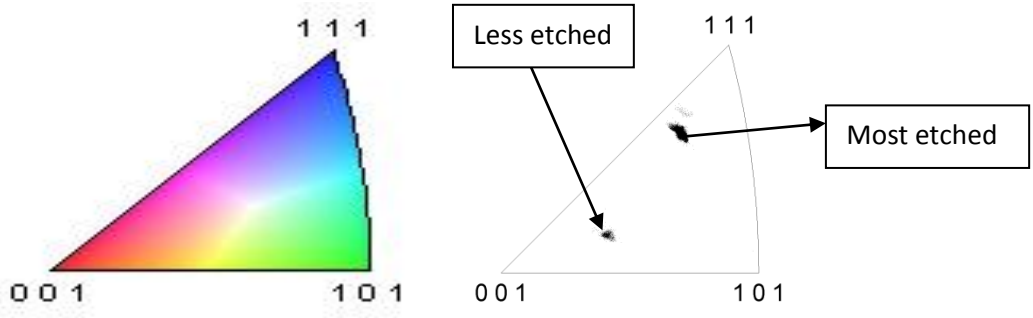

Figure 4.1.2.d: Figure showing the inverse pole figure (left) that is being used to determine the crystallographic orientation of grains investigated by EBSD. The right figure shows where most of the test points ended during the EBSD analyses don on the surface shown in figure 4.1.2 c.

4.1.3 Height and roughness measurements

Roughness measurements done on neighboring grains in the pure aluminum samples etched in 1.25 molar NaOH at 70°C for 10 minutes showed a different roughness between grains close to the [111] orientation compared to grains closer to the [001] and the [101] orientation. In table 4.1.3.a a representative results from 5 measurements done on grains showing the same crystallographic orientation as in figure 4.1.3.a can be seen. It is clear that grain having a crystallographic orientation closer to the [111] orientation has a lower root mean square (R_q) and average distance from profile centerline (R_a) than the grains that is closer to the [001] crystallographic orientation. By comparing the roughness results from the pure aluminum against the roughness results from the AlCu1000-alloy (table 4.1.3.b) it can be seen that the copper containing aluminum has both a higher R_q and R_a values for all the crystallographic orientations tested. The copper containing aluminum shows a lower roughness for the less etched grains compared to the pure aluminum that shows the opposite result.

To create the roughness graphs for each grain the software uses the most common height found in each grain and sets this as a zero point for the test. Then the height of each point of the investigated area is plotted compared to the zero point found. Figure 4.1.3.b, c-g shows the surface roughness along paths tested on the surface of figure 4.1.3 a, and 4.1.3.d compared to the zero point set by the software. It can clearly be seen that the less etched grain on the pure aluminum has higher peaks compared to the more etched grain, graphs from the AlCu1000 alloy shows the opposite result.

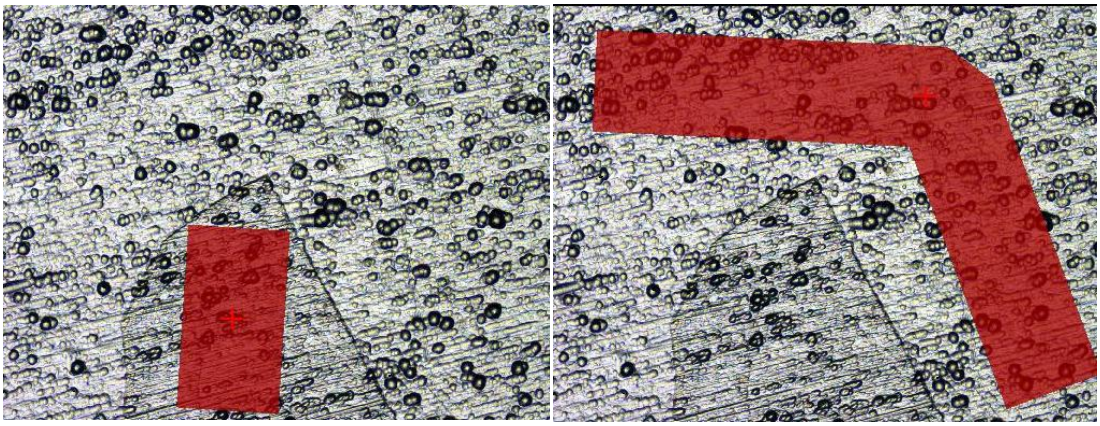

Figure 4.1.3.a: Pictures showing area tested on a pure aluminum sample etched in 1.25 molar NaOH solution for 10 minutes at 70°C. Left picture shows the area tested on the most etched grain. Right picture shows the area tested for the less etched grains.

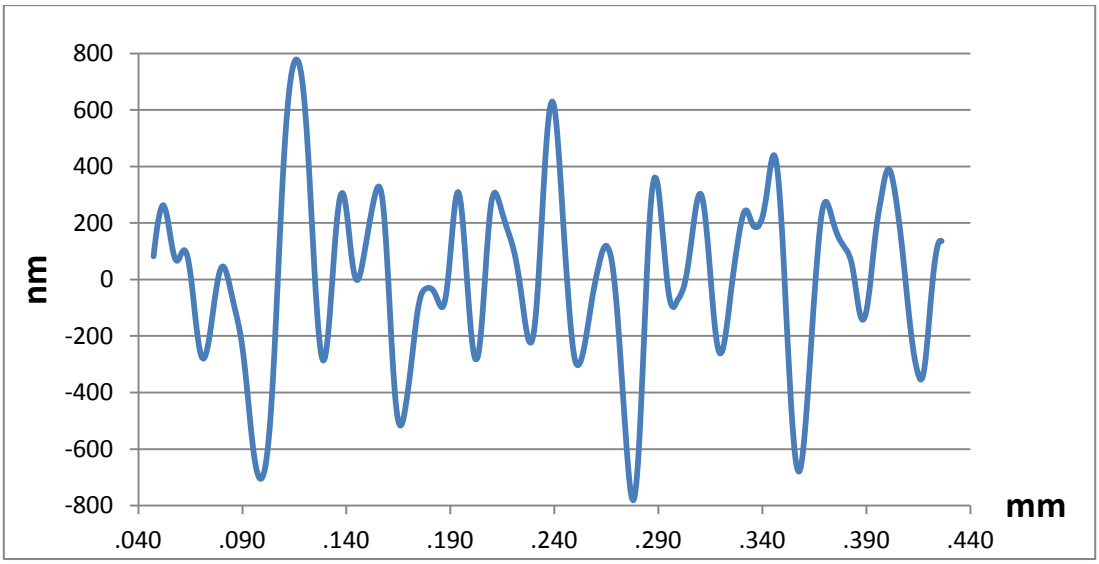

Figure 4.1.3.b: Graph showing the roughness of the most etched grain on the pure aluminum surface shown in the left picture in figure 4.1.3.a.

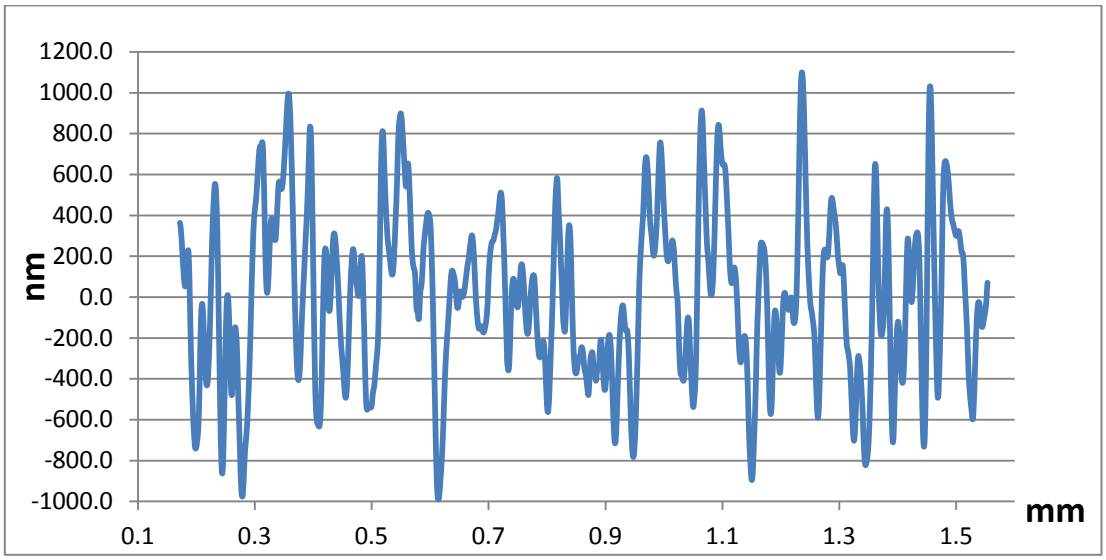

Figure 4.1.3.c: Graph showing the roughness of the less etched grains on the pure aluminum surface shown in the right picture in figure 4.1.3.a.

Table 4.1.3.a: Table showing representative results from 5 roughness measurements done on pure aluminum showing the same etched surface as in figure 4.1.3.a. Etching has been done in 1.25 molar NaOH at 70°C for ten minutes.

	R_q [µm]	R_a [µm]
Highly etched	1.0±0.1	0.8±0.1
Low etched	1,7±0.1	1.3±0.1

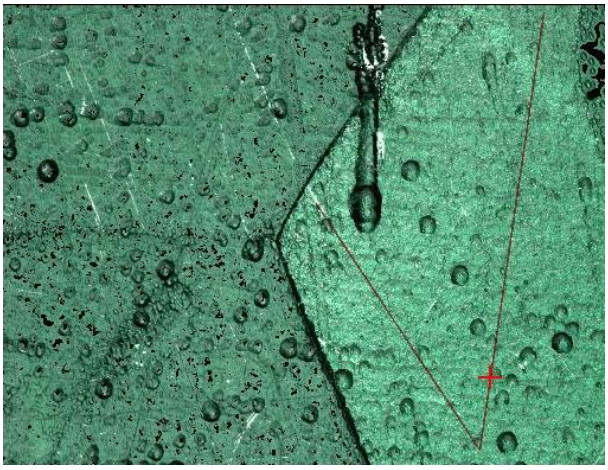

Figure 4.1.3.d: Pictures showing the three different grains that have been used for roughness measurements on an AlCu1000-alloy. On the picture, the right grains have etched less than the two grains to the left. The picture gives a representative image and measurements for roughness and height measurements on AlCu1000-alloys.

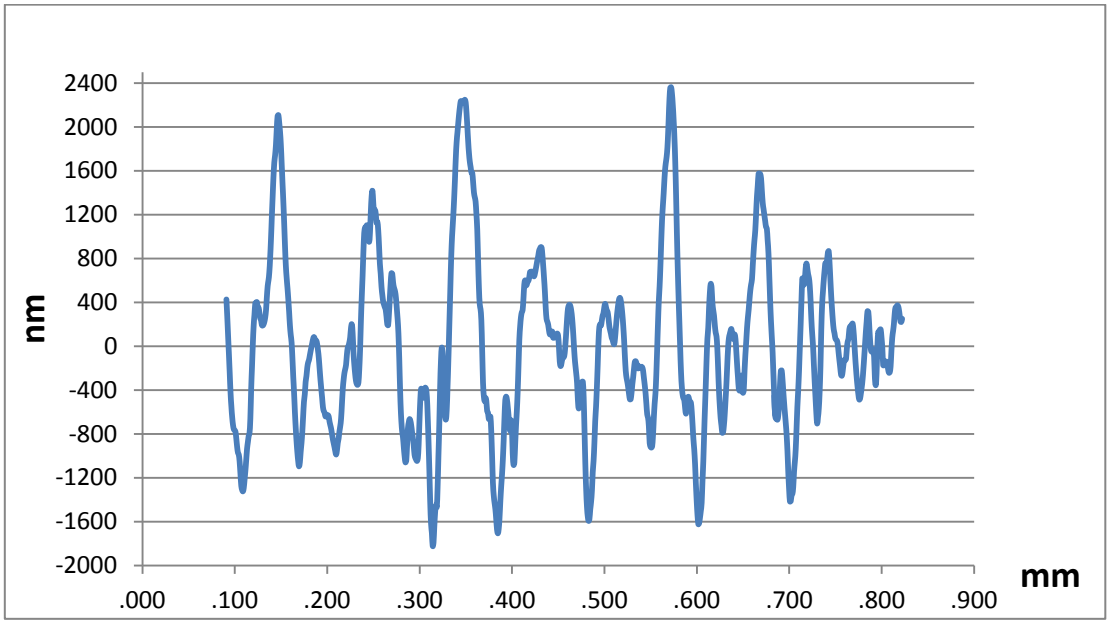

Figure 4.1.3.e: Graph showing the roughness measured on the right grain in figure 4.1.3.d.

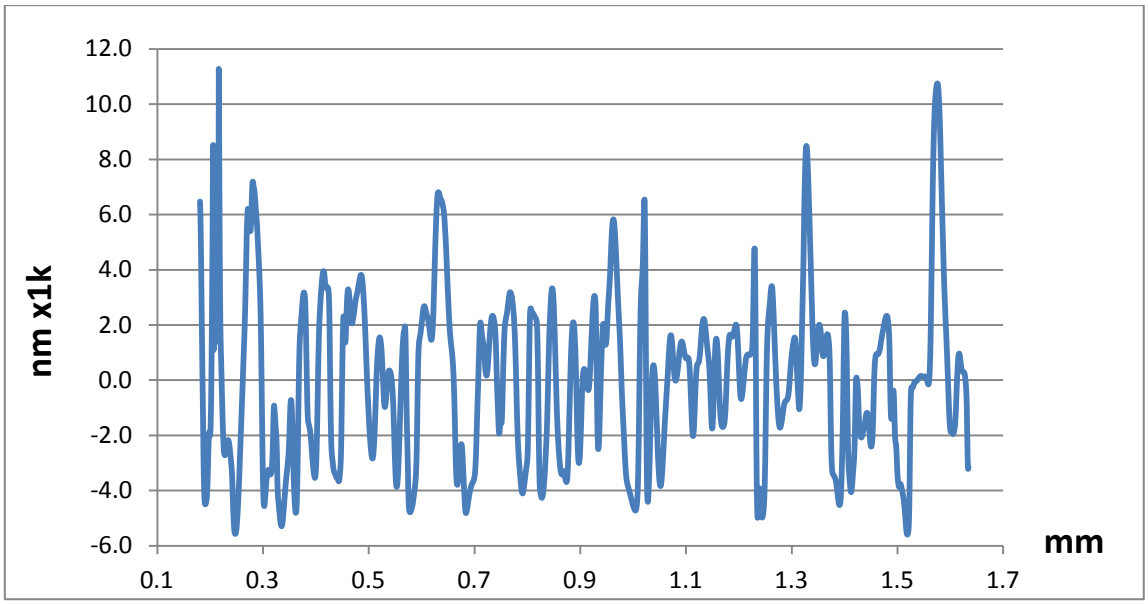

Figure 4.1.3.f: Graph showing the roughness measured on the upper left grain in figure 4.1.3.d.

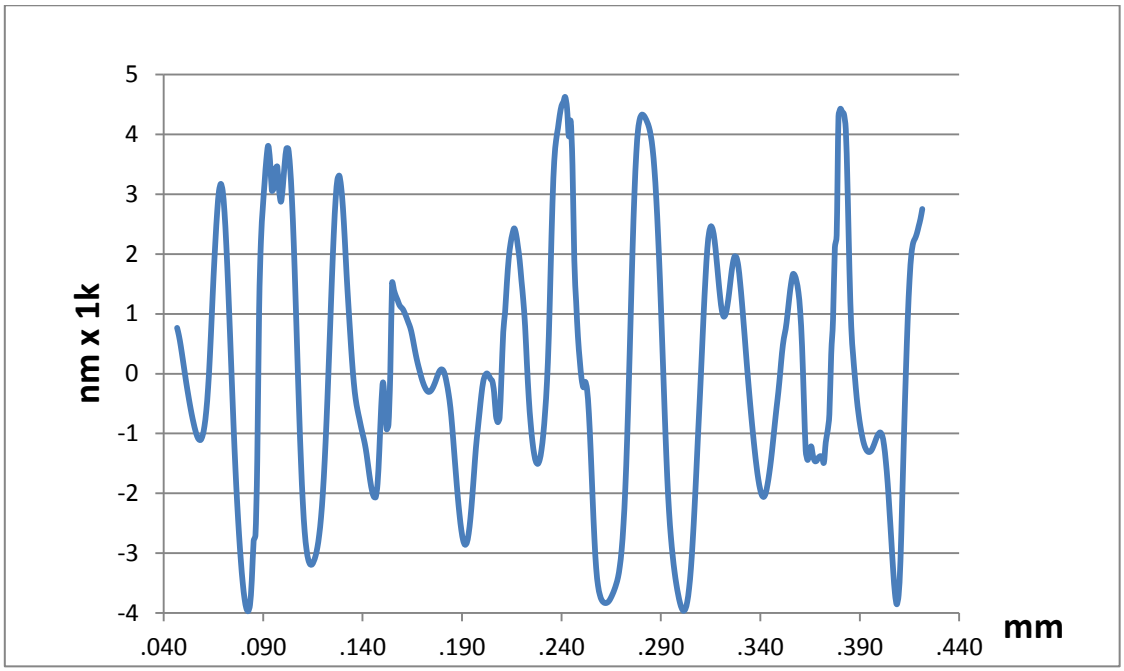

Figure 4.1.3.g: Graph showing the roughness measured on the lower left grain in figure 4.1.3.d.

Table 4.1.3.b: Table showing representative R_q and R_a values measured on 7 different areas on AlCu1000-alloys containing 3 differently etched grains equal to figure 4.1.3.d.

	R_q [µm]	R_a [µm]
Right grain	0.8±0.2	0.6±0.1
Lower left grain	2.3±0.2	1.6±0.1
Upper left grain	3.4±0.1	2.3±0.1

Height differences measured between the different grains investigated on the pure aluminum and the Alcu1000-alloy shows that there is a clear difference in the etching rate between grains showing different crystallographic orientation. From table 4.1.3.c there can be seen that the average height difference between the less etched and the most etched grains in the pure aluminum etched at 70°C for 10 minutes lies between 1µm and 1, the average have been measured from 5 different areas. The variance in the height results depends on how close the grains are to the [111] and the [001] orientation. The AlCu1000-alloys also show a higher etching rate for grains that has a crystallographic orientation closer to the [111] orientation compared to the [001] orientation after etching. But by comparing the results against the pure aluminum it can be seen that the etching rate is much higher with copper in the alloy. Table 4.1.3.d shows a representative average height difference from 12 measurements done on neighboring grains in AlCu1000-alloys.

Table 4.1.3.c: Table showing the height difference between the less etched and the most etched grains investigated on pure aluminum etched in 1.25 molar NaOH for 10 minutes at 70°C. The variance shown is the average variance taken from 5 measurements done on pure aluminum.

Alloy	Etched grain [µm]	Less etched [µm]
pAl	1.0±0.5	0.0±0.5

Table 4.1.3.d: Table showing the height difference between the less etched and the most etched grains investigated on aluminum containing 1000 ppm copper etched in 1.25 molar NaOH for 10 minutes at 70°C. The variance shown is the average variance taken from 12 measurements done on AlCu1000 alloys.

Alloy	Less etched[µm]	Most etched[µm]	Less etched [µm]
AlCu1000	0.0±0.5	5.0±1.0	2.5±1.0

4.1.4 Energy Dispersive Spectroscopy (EDS)

Results from Electron Diffraction Spectroscopy (EDS) tests done on AlCu1000 specimens that have been etched in NaOH can be seen in figure 4.1.4.a and figure 4.1.4.b. The two tests are taken on one highly etched grain, figure 4.1.4.a, and one less etched grain, figure 4.1.4.b. The figures give a good representation of several tests done on etched AlCu1000 specimen. As seen in the figures, little or no differences can be seen from the highly etched grain to the less etched grain. Both the tests show high aluminum peaks, ~375 cps[6] as well as clear peaks for oxygen and copper. The only difference between the highly etched grain and the less etched grain is that the oxygen peak is slightly higher, ~0.5 cps for the more etched grain. A clear peak around 3keV can be seen in all tests done on AlCu1000 alloys. This peak indicates that there is Ag on the surface of the test specimens, something that is not possible. When taking a closer look at the figures it can be seen that the 3 keV peaks are about two times the energy of aluminum (~1.5 keV), indicating that there have been errors in the counting rate of aluminum so that two aluminum particles have been counted as one and therefore creating a 3 keV peak (~1.5x2).

[6] Cps=counts per second

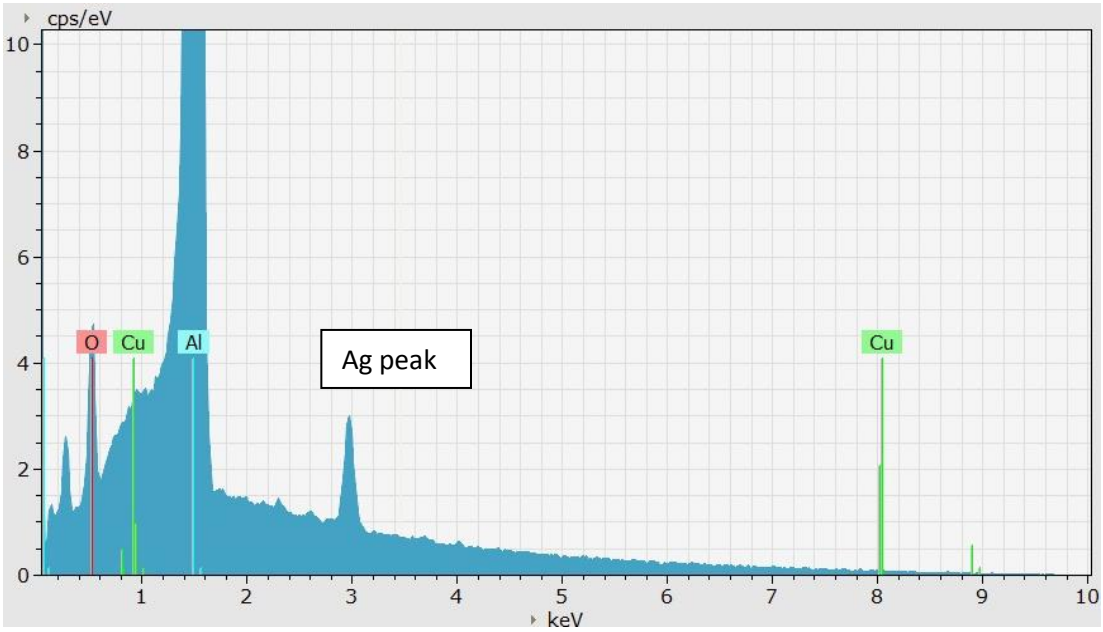

Figure 4.1.4.a: Graph showing EDS result from a highly etched grain on the surface of an AlCu1000 alloy etched in NaOH

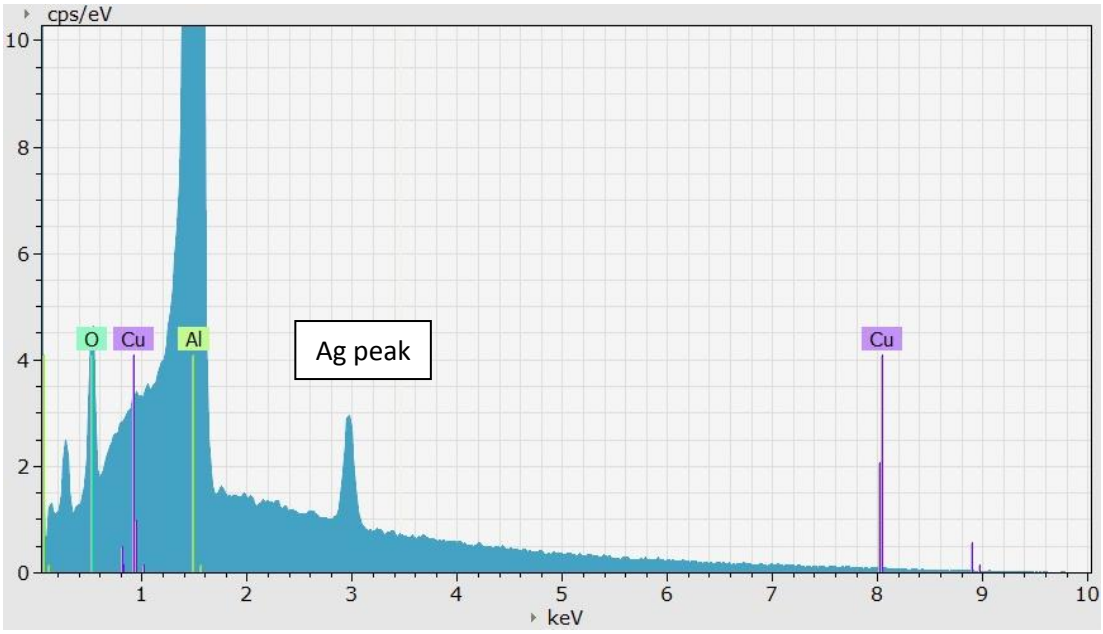

Figure 4.1.4.b: Graph showing EDS result from a less etched grain on the surface of an AlCu1000 alloy etched in NaOH

4.1.5 Corrosion potential

From the corrosion potential tests done at 25°C it can clearly be seen from figure 4.1.5.a that after 1000 seconds the four alloys shows a clear difference in their corrosion potential. An increasing amount of copper in the aluminum alloy increases the corrosion potential and after 5400 seconds the potential of all the alloys started stabilizing. At the end of the test pure aluminum showed -1.48V, AlCu10 showed -1.44V, AlCu100 showed -1.41V, and the AlCu1000 showed -1.38V vs. HG/HgO. It can also be seen from figure 4.1.5.a that in the initiation time of the experiment (the first 5 seconds) the AlCu10 alloy shows the lowest corrosion potential (-1.88V vs. Hg/HgO) compared to the other test specimens. Aluminum alloyed with 100 and 1000 ppm copper shows the highest corrosion potential from 7 seconds trough out the entire experiment. The bottom for each graph (lowest potential) indicates the point where the oxide film has become sufficiently thin so that the bulk material can corrode. The reason for the increasing potential after the lowest point is due to surface enrichment of copper and other impurities from the alloy. By increasing the temperature of the etching bath from 25°C to 70°C the corrosion potential of all the test specimens decreases as seen in figure 4.1.5.b. Due to lower adhesion between the specimen surface and the paint used to limit the surface are during higher temperatures, the 70°C tests showed signs of etching under the paint after about 300 seconds limiting the test period to 1000 seconds where the test area started to become larger than at the start of the experiment. After 300 seconds the pure aluminum showed -1.75V, Alcu10 showed -1.74V, AlCu100 showed -1.72V, and the AlCu1000 showed -1.62V vs. Hg/HgO. In the initiation time (5-10 seconds) of the 70°C test the pure aluminum and the AlCu10 showed the same signs as in the 25°C test, only with a slightly lower corrosion potential (-1.93V vs. Hg/HgO for the pure aluminum and -1.92 V vs. Hg/HgO for the AlCu10). The biggest difference in the initiation time was found for the AlCu100-alloy that showed -1.58 V.vs. Hg/HgO after 5-10 seconds at 25°C and -1.92 V vs. Hg/HgO in the 70°C test. The clear difference between the four alloys could also be seen earlier in the 70°C test (after 40 seconds) compared to in the 25°C test (250 seconds).

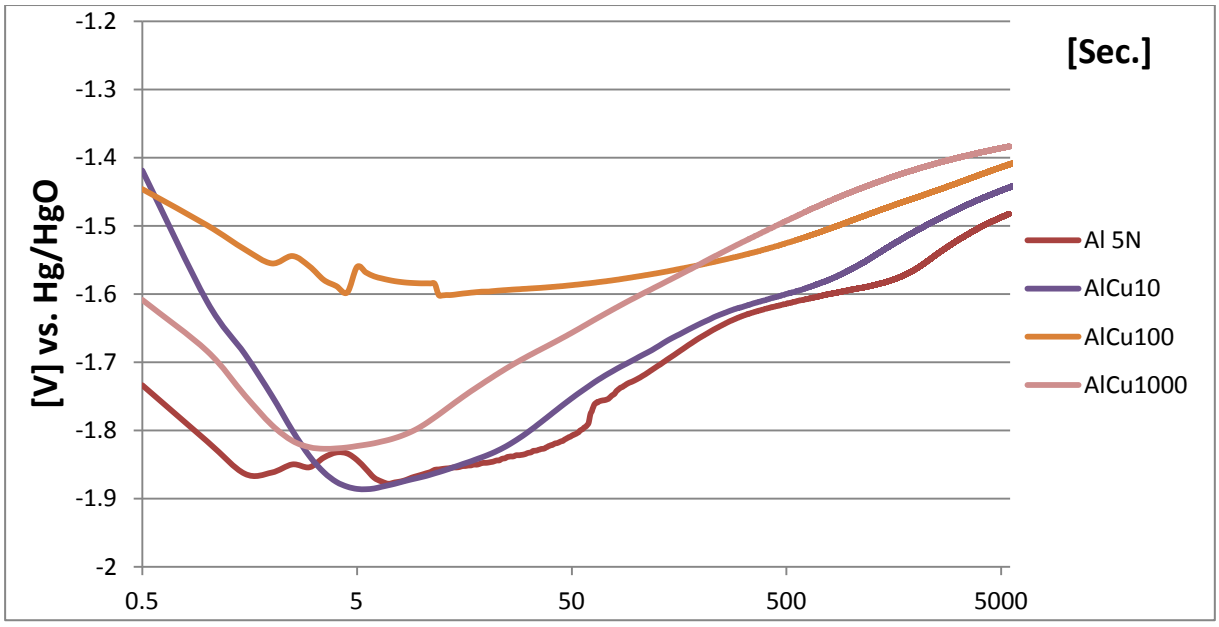

Figure 4.1.5.a: Graph showing the corrosion potential measurements done in 1.25 molar NaOH at 25°C.

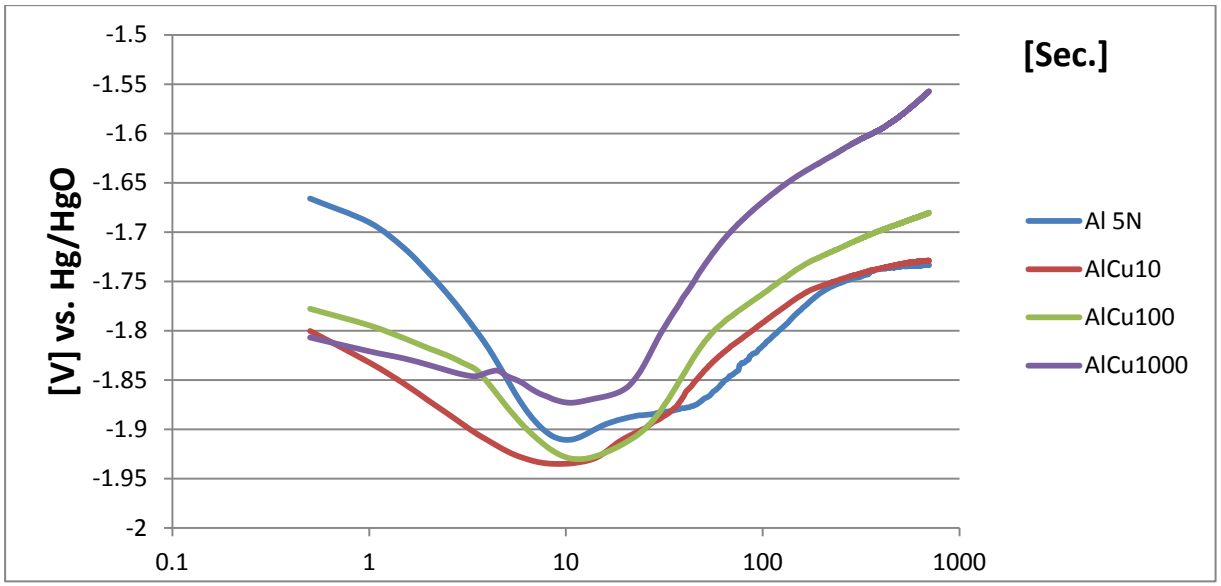

Figure 4.1.5.b: Graph showing corrosion potential measurements done in 1.25 molar NaOH at 70°C.

4.2 GD-OES results

The GD-OES results shown come from quantitative data. Parameters used in the GD-OES tests and the results from AlCu10-alloys are shown in appendix D.

4.2.1 Pure Aluminum

GD-OES tests done on pure aluminum that has been etched in 1.25 molar NaOH solution at 25°C for six hours and desmutted in nitric acid after being etched (figure 4.2.1.b) shows small amounts of copper and iron close to the surface of the oxide layer. The test specimen that has not been desmutted after etching (figure 4.2.1.a) shows a higher amount of both copper and iron in the oxide layer close to the oxide/bulk material border. Graphs created from GD-OES tests done on pure aluminum that has been etched at 70°C and desmutted show a slightly higher content of copper and iron in the oxide layer than the specimen etched at 25°C, this is not the case for the specimen etched at 70°C that has not been desmutted after etching. The copper and iron peaks occur behind the oxide layer and they are both lower than the copper and iron peaks shown in the 25°C etched aluminum that not has been desmutted. It can also be seen that the oxide layer of the 70°C etched specimen that has not been desmutted are thinner than for the specimen etched at 25°C.

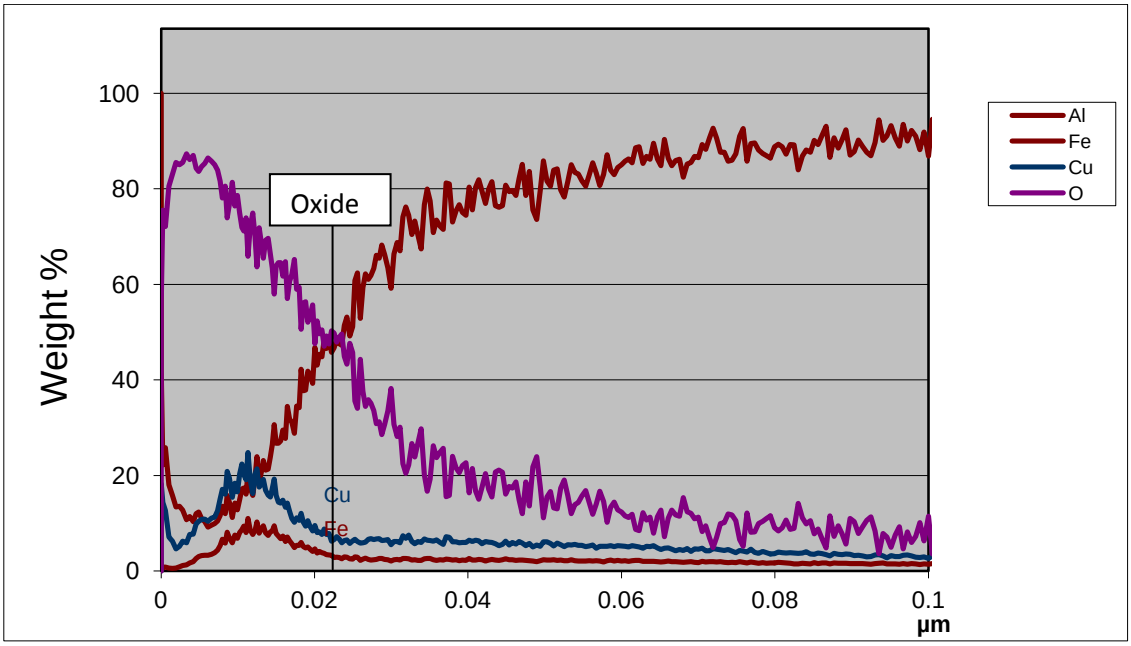

Figure 4.2.1.a: Graph showing the first 0.1µm of the GD-OES test done on pure aluminum that has been etched at 25°C without being desmutted in nitric acid after etching. Cu graph have been multiplied by 10.

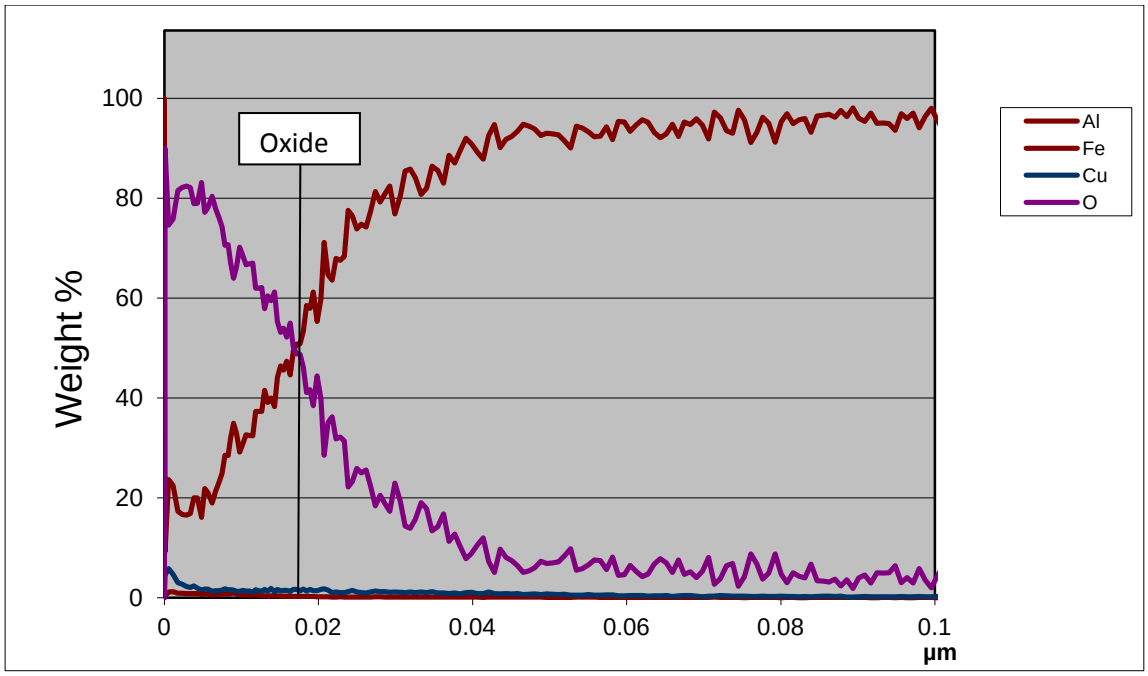

Figure 4.2.1.b: Graph showing the first 0.1µm of the GD-OES test done on pure aluminum that have been etched at 25°C and desmutted in nitric acid. Cu graph have been multiplied by 10.

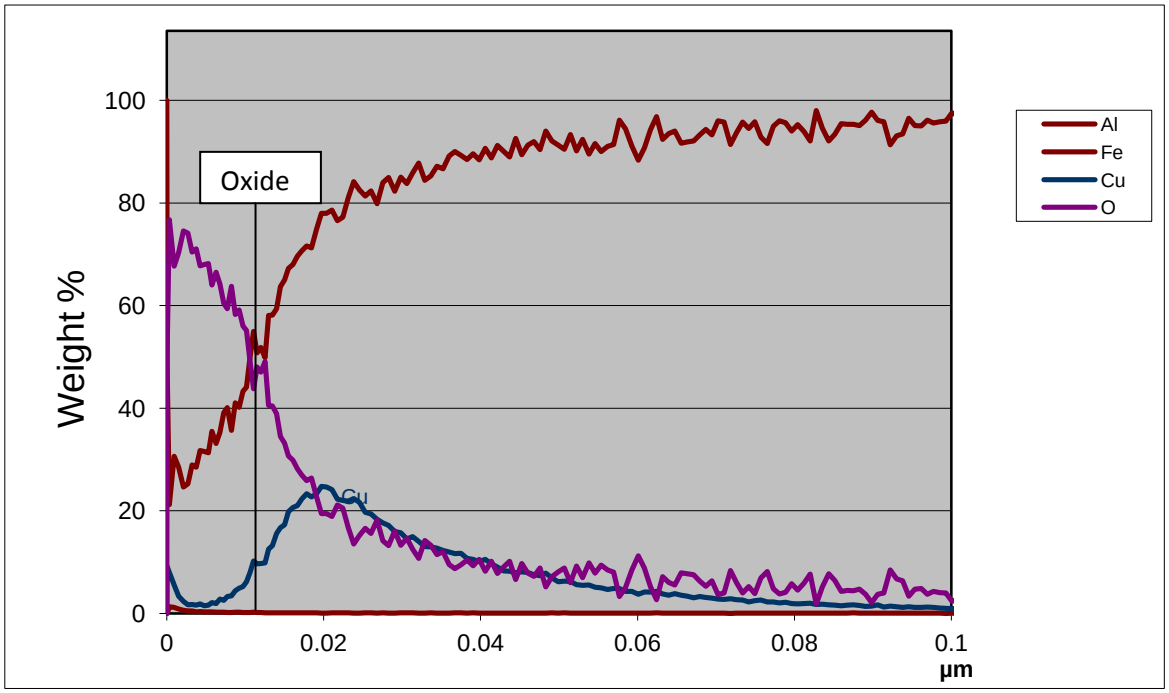

Figure 4.2.1.c: Graph showing the first 0.1µm of the GD-OES test done on pure aluminum that has been etched at 70°C without being desmutted in nitric acid after etching. Cu graph have been multiplied by 10.

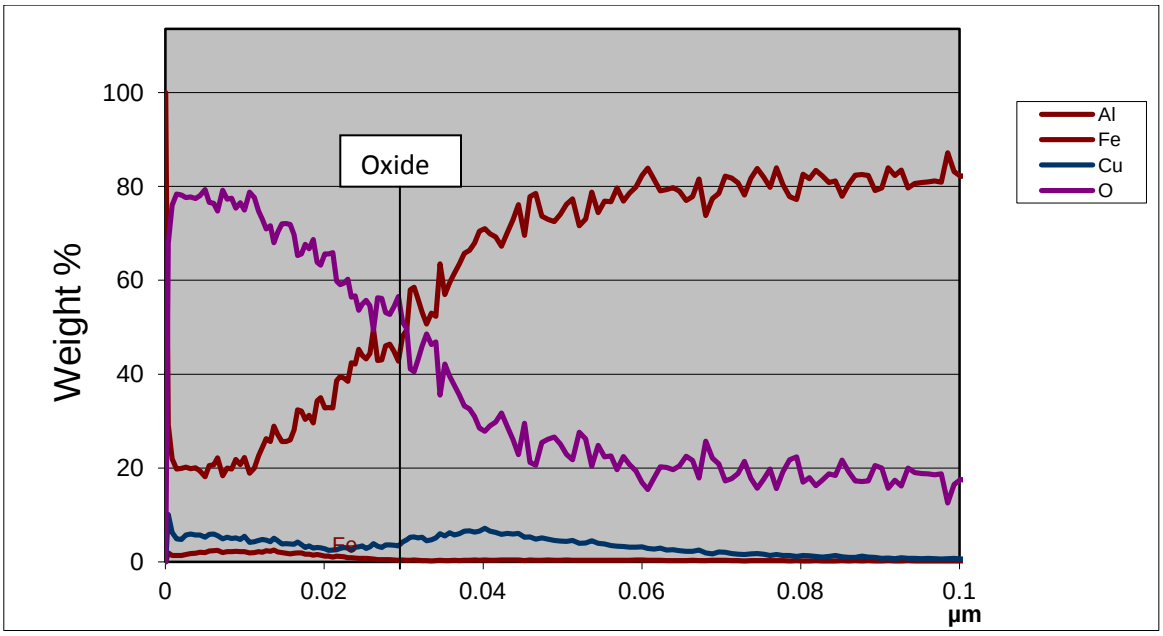

Figure 4.2.1.d: Graph showing the first 0.1µm of the GD-OES test done on pure aluminum that have been etched at 70°C and desmutted in nitric acid after etching. Cu graph have been multiplied by 10.

4.2.2 1000 ppm copper

GD-OES tests done on AlCu1000 alloys that have been etched at 25°C for one hour shows an increased amount of copper in the outer part of the oxide film compared to the copper amount in the bulk material. The specimen that have been desmutted after being etched shows a slight dip and a slightly smaller copper amount in the outer 0.005 µm of the oxide film compared to the specimen that hot have been desmutted. It is also possible to see that the oxide layer is slightly thicker for some of the desmutted specimen. By increasing the temperature of the etching bath from 25°C to 70°C and etching for 1 hour the copper amount in the oxide layer increased with about 3-5% for both the desmutted and the not desmutted specimen. It is also possible to see that the oxide layer becomes thinner. For the tests done at 70°C etched specimen no signs of a thickness difference of the oxide layers could be detected between not desmutted and desmutted samples. By comparing the GD-OES results from the pure aluminum to the results from the AlCu1000 alloys it is possible to see that there are no signs of iron in the oxide layer of the AlCu1000 test specimens.

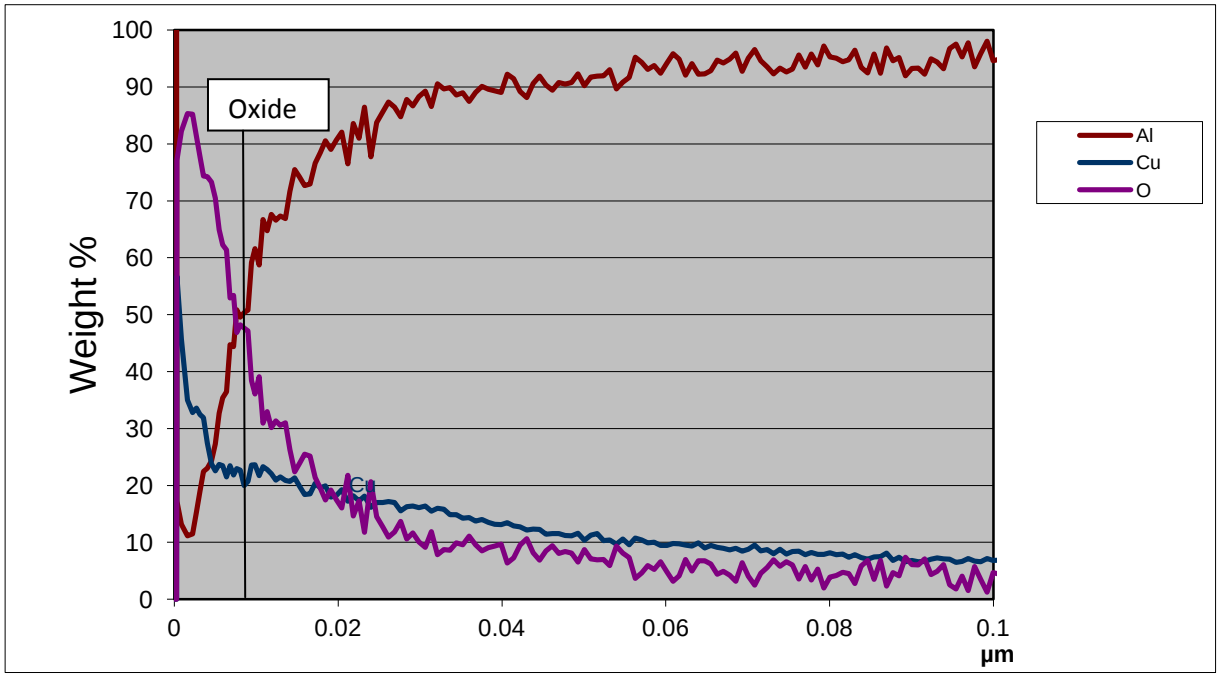

Figure 4.2.2.a: Graph showing the first 0.025µm of the GD-OES test done on AlCu1000 alloy that has been etched at 25°C without being desmutted in nitric acid after etching. Cu graph have been multiplied by 10.

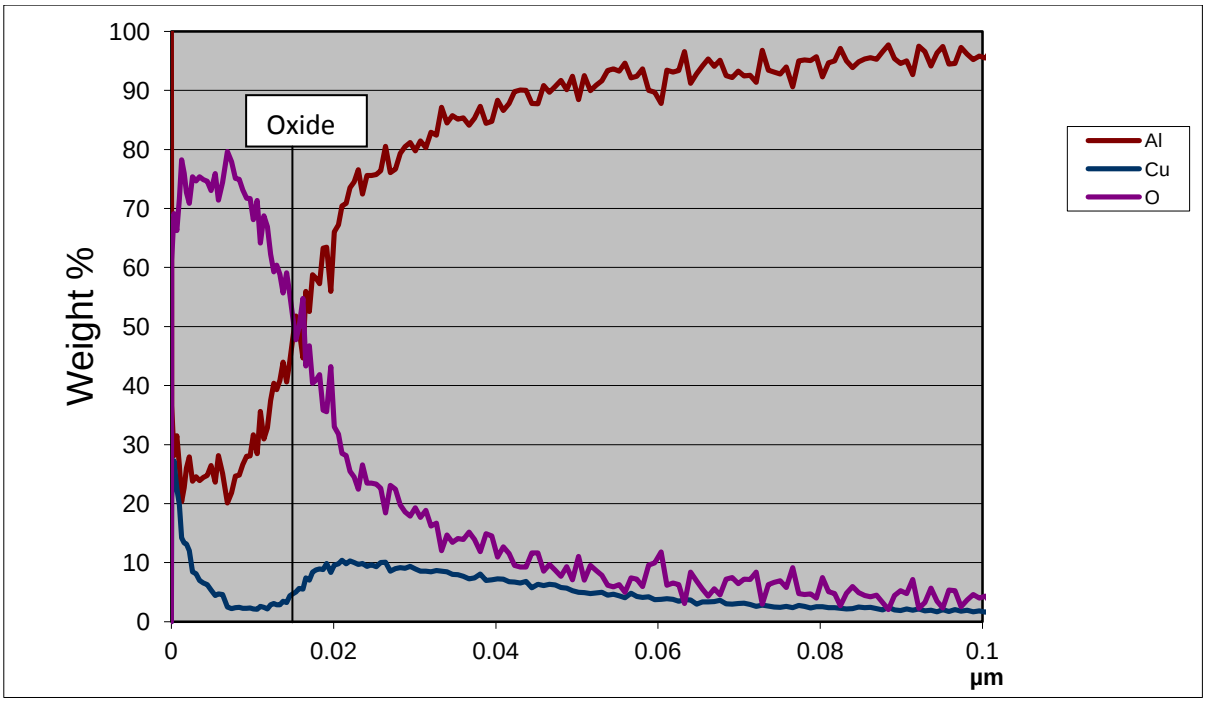

Figure 4.2.2.b: Graph showing the first 0.025µm of the GD-OES test done on AlCu1000 alloy that have been etched at 25°C and desmutted in nitric acid. Cu graph have been multiplied by 10.

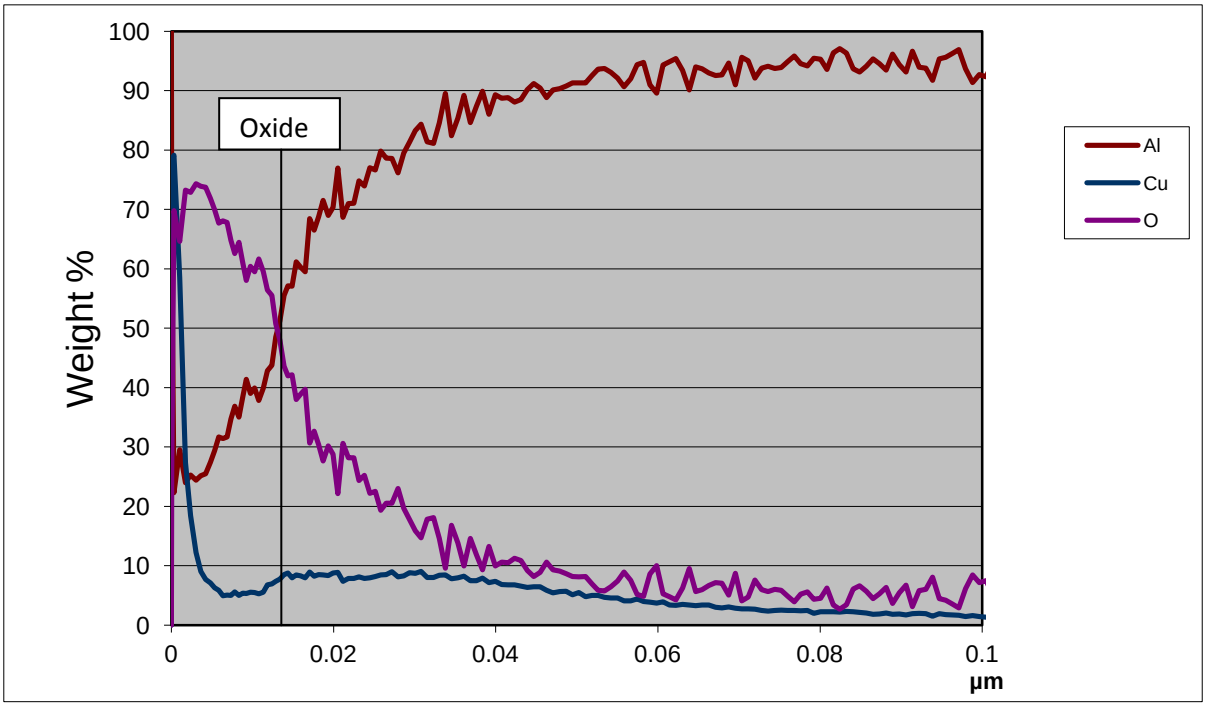

Figure 4.2.2.c: Graph showing the first 0.025µm of the GD-OES test done on AlCu1000 alloy that have been etched at 70°C and desmutted in nitric acid. Cu graph have been multiplied by 10.

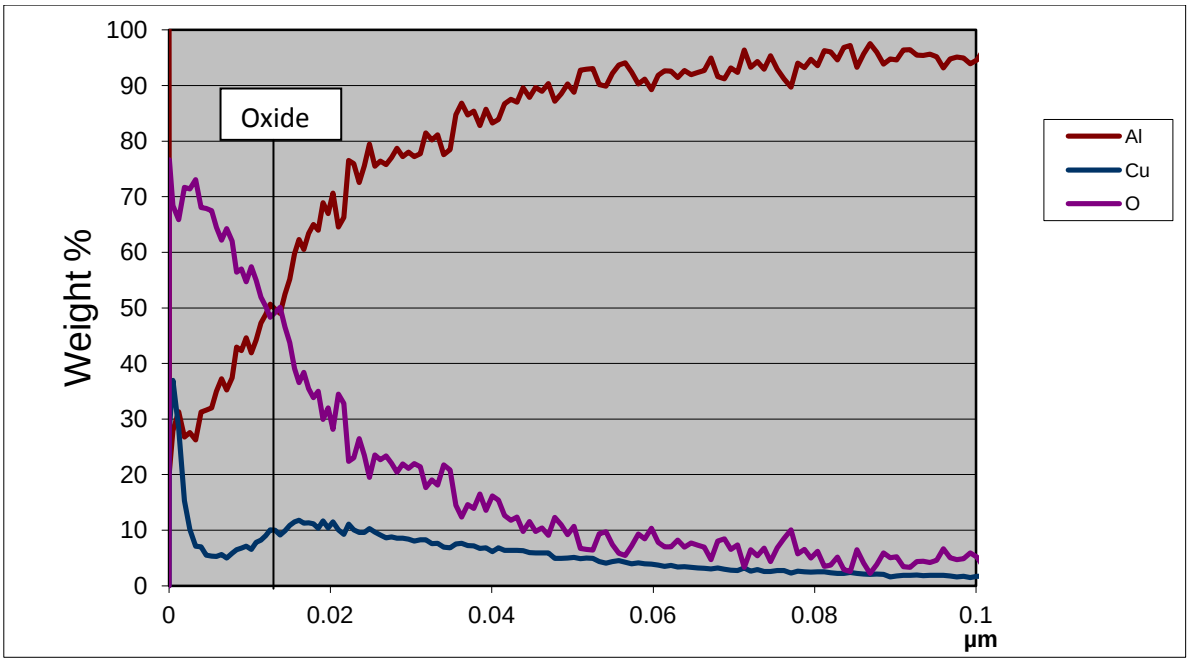

Figure 4.2.2.d: Graph showing the first 0.025µm of the GD-OES test done on AlCu1000 alloy that has been etched at 70°C without being desmutted in nitric acid after etching. Cu graph have been multiplied by 10.

4.3 Acid etch

4.3.1 Etch rate

Weight loss tests done using HCl as an etching media showed little or no etching of the pure aluminum, AlCu10, and AlCu100 for the first few hours. After 6 hours some hydrogen development on the AlCu100 could be seen in the 1.3 molar solution. After 12 hours the pure aluminum did not show any signs of corrosion while the AlCu10 and AlCu100 showed small signs of corrosion on the surface, but not enough to see the grain structure. Further, the AlCu1000-alloy showed signs of hydrogen development after 3 hours and even more hydrogen development after about 7 hours. There could clearly be seen that some areas on the surface was creating more hydrogen than the rest of the specimen indicating that certain grains corroded more than others, but no remarkable height differences could be measured.

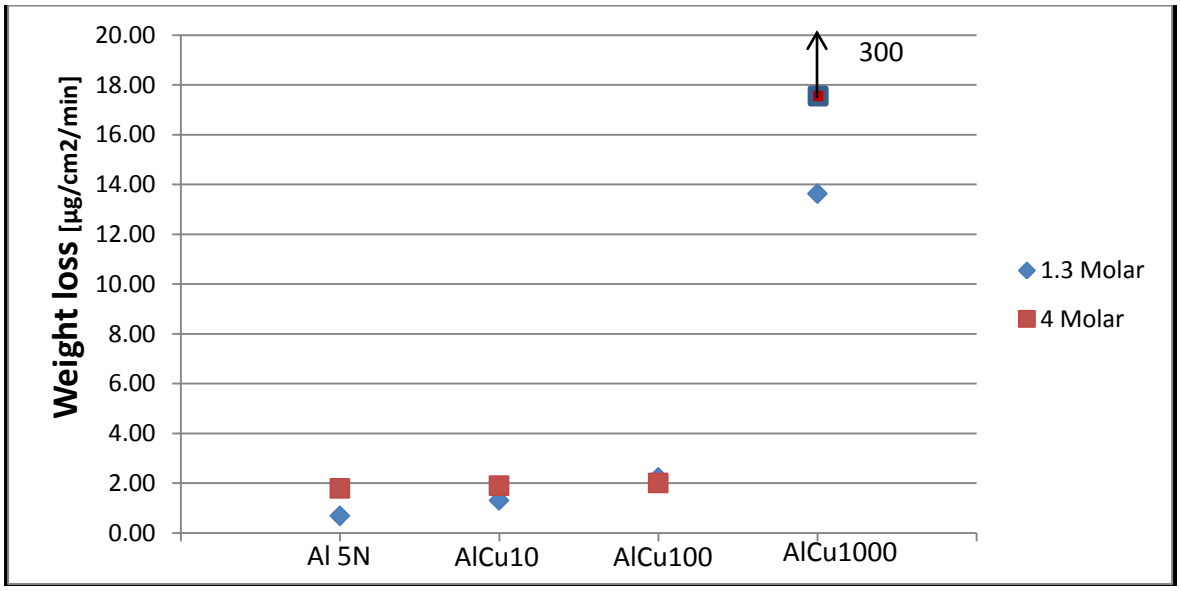

Figure 4.3.1.a: Graph showing the average (µg/cm^2/ min) etching rate for the 1.3 molar and 4 molar experiments. No remarkable differences occur in the etching of Al 5N, AlCu10, and AlCu100 for the two solutions.

The test done using 4 molar HCl solution showed little or no etching of the pure aluminum and the AlCu10-alloy trough out the testing period, some hydrogen development could be seen on the surface of the AlCu10-alloy at the end of the test. The AlCu100-alloy showed a higher hydrogen development than the pure aluminum and the AlCu10-alloy 3 hours into the test, but no remarkable weight loss could be detected compared to the pure aluminum. As for the AlCu1000-alloy a clear hydrogen development in certain areas on the test specimen could be seen after about 240 minutes of testing, this development increased slightly until about 300 minutes. And after about 310 minutes the hydrogen development increased drastically showing a high development on the entire test specimen. The etching bath changed color from clear to grey and the temperature of the 200 ml bath increased from 25°C to 29°C in 25 minutes. This high etching rate continued for about 75 minutes before the temperature of the bath started falling towards 26.5±0.5°C, the hydrogen development also slowed down but the bath still looked like it was boiling. After the test using 4 molar HCl was done no remarkable etching of the surface of the pure aluminum, AlCu10, and the AlCu100 could be seen with the naked eye. As for the AlCu1000 specimens they had changed from a metallic looking surface to a dull black/grey surface that looked like it was covered with some type of dust. In figure

4.3.1.b it is possible to see how the surface of the AlCu1000 looked like after being desmutted in nitric acid.

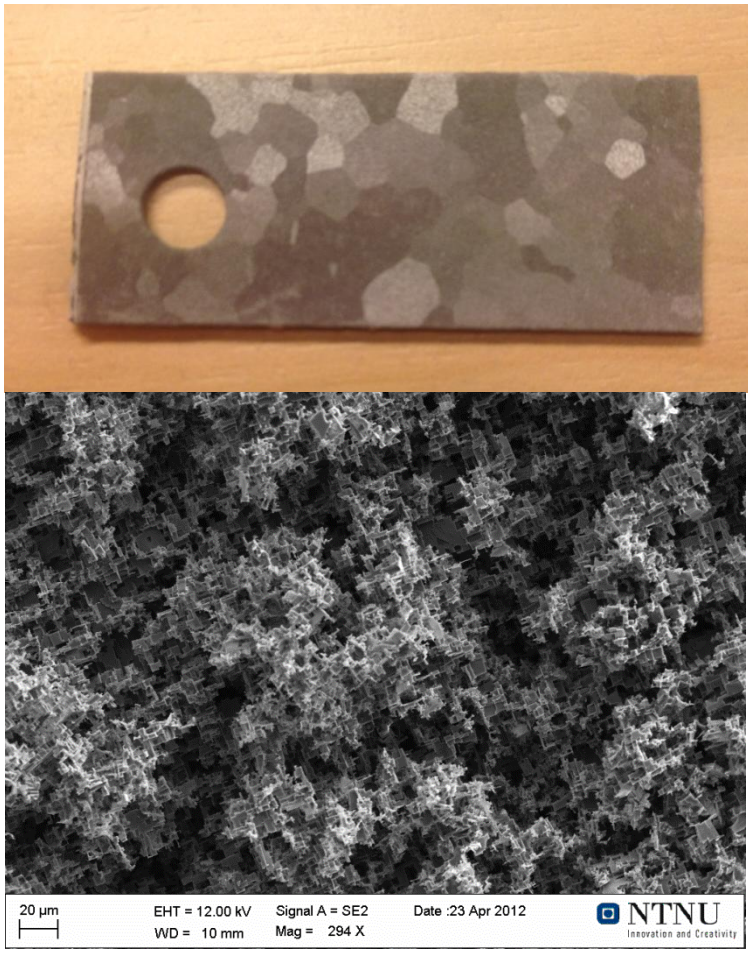

Figure 4.3.1.b: Top picture showing AlCu1000 test specimen after being etched using 4 molar HCl for 6 hours. Bottom picture shows a SEM photo of the porous and rough surface on the AlCu1000 test specimen.

4.3.2 Roughness and height measurements

For the height and roughness measurements of the HCl etched test specimens only the AlCu1000-alloy was investigated due to the small or no etching of the other alloys. Both height difference between neighboring grains and the roughness of the grains was investigated before the surface layer (figure 4.3.1.b) was attempted removed. As seen in table 4.3.2 the roughness of the grains investigated changed with the crystallographic orientation and the [111] grains had a slightly low roughness than grains that was closer to the [001] and [101] planes. But no big differences were detected due to the surface layer. Removing the layer was den tried using 65% nitric acid at 25^{o}C and Chrome Phosphoric acid at 90^{o}C without any result. Further a 1.25 molar NaOH solution was used at 25^{o}C to remove the surface layer. The porous nature of the layer made this a problem since etching of the underlying bulk material also might happen during etching of the surface layer. After 10 minutes of etching the layer was gone indicating that the layer had an average thickness of around 5 µm, calculated from the average etching rate per minute of AlCu1000 in 1.25 molar NaOH at 25^{o}C. But by looking at figure 4.3.1.b it can be seen that the thickness of the layer probably is much higher.

Table 4.3.2: Table showing roughness measured in several grains etched in 4 molar HCl at 25°C. Grains that lie in the center between two crystallographic orientations are noted with the two orientations they lie between.

Tested grain	R_q [µm]	R_a [µm]	Closest crystallographic orientation
Cu1000	3.2±0.2	2.5±0.2	[111],[001]
Cu1000	3.0±0.9	2.3±0.7	[111]
Cu1000	3.4±0.05	2.7±0.03	[001]

Height differences between neighboring grains was measured before the surface layer was removed but no measurable height differences could be detected between grains having [111] and [001] orientations. After etching the test specimens using 1.25 molar NaOH for 1 minute at 25°C a height difference for about 16 µm could be measured between grains showing [111] and [001] crystallographic orientations. But due to the use of NaOH for removing the surface layer this result cannot be regarded as a correct result for the acidic etching experiment.

4.3.3 Electron Diffraction Spectroscopy (EDS)

Electron Diffraction Spectroscopy (EDS) measurements of the surface layer that developed during etching of AlCu1000 was done on several grains showing different heights to detect the elements occurring in the layer. Figure 4.3.3 shows a representative graph from EDS measurements done on several specimens but no big differences could be detected from these tests compared to the EDS tests done on AlCu1000-alloys etched in NaOH. A probable reason for this is because the volume tested reaches beneath the surface layer so that the bulk material also affects the peaks in the graph A slightly higher amount of oxygen was detected for all the tests, but no big differences in the amount of copper could be detected. Also here the peak at 3keV could be detected, but also here this is probably just a double detection of aluminum.

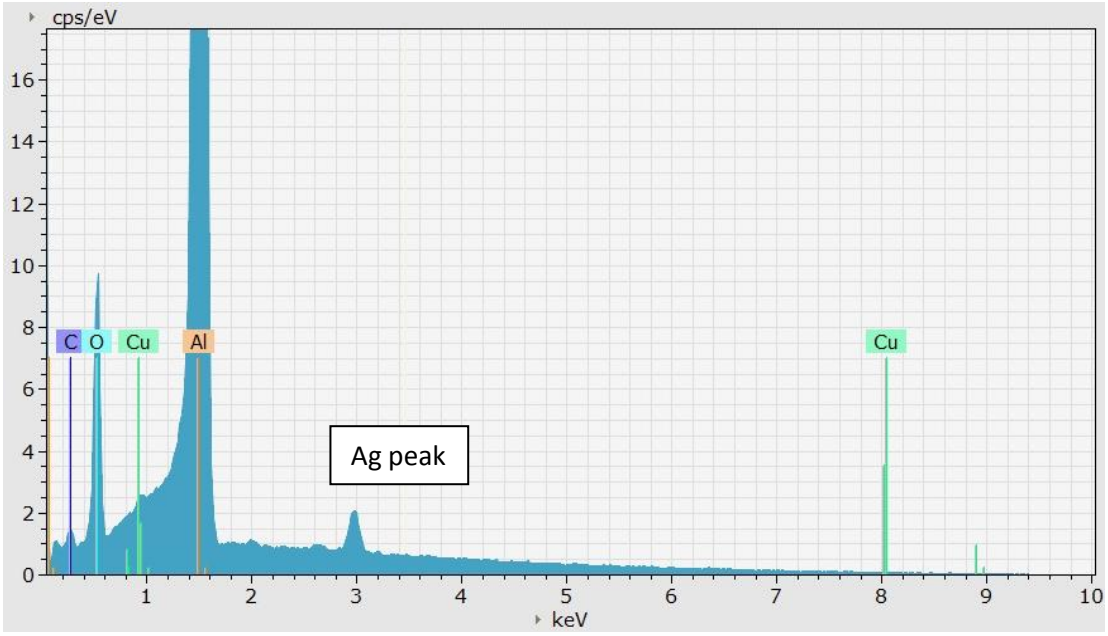

Figure 4.3.3: Graph showing EDS result from the surface layer developed on AlCu1000 alloys that have been etched in HCl acid.

4.3.4 Corrosion potential

From the corrosion potential graph in (figure 4.3.4.a) it can be seen that an increasing copper amount in the alloy increases the corrosion potential. On the red line representing the AlCu1000-alloy it can be seen changes in the graph after ~50 seconds and after ~700 seconds. These changes indicate a increase in the hydrogen development on the surface. After 50 seconds hydrogen development on the surface started showing, at 700 seconds the development increased drastically as the temperature in the bath started increasing and the color of the bath changed from clear to gray. After about 800 seconds the test specimen had etched so badly that it was almost gone and the lowest part of the "dip" at 1000-1100 seconds indicate the point where the specimen was entirely gone. The pure aluminum sample showed a stable potential the first 100 seconds before it started increasing from-0.87 V vs. Hg/HgO towards -0.975 V vs. Hg/HgO. This point indicates where the oxide layer is thin enough for the bulk material to oxidize. After 8000 seconds the potential started decreasing back towards -0.87 V vs. Hg/HgO before it stabilized at this point until the test was stopped at 60500 seconds. After the corrosion potential test the pure aluminum did not show any remarkable signs of being exposed for 4 molar HCl acid for almost 17 hours. Pictures of the test specimens after being tested can be seen in figure 4.3.4.b. Two tests of the AlCu1000-alloy was done, one where the surface of the HCl acid was on the line between the paint and the aluminum surface (Cu1000-S), and one where the surface of the HCl was on the middle of the paint (Cu1000). This was done to see if the result would be different due to the higher etching rate closer to the surface of the etching media where there are much more oxygen than further down into the etching bath.

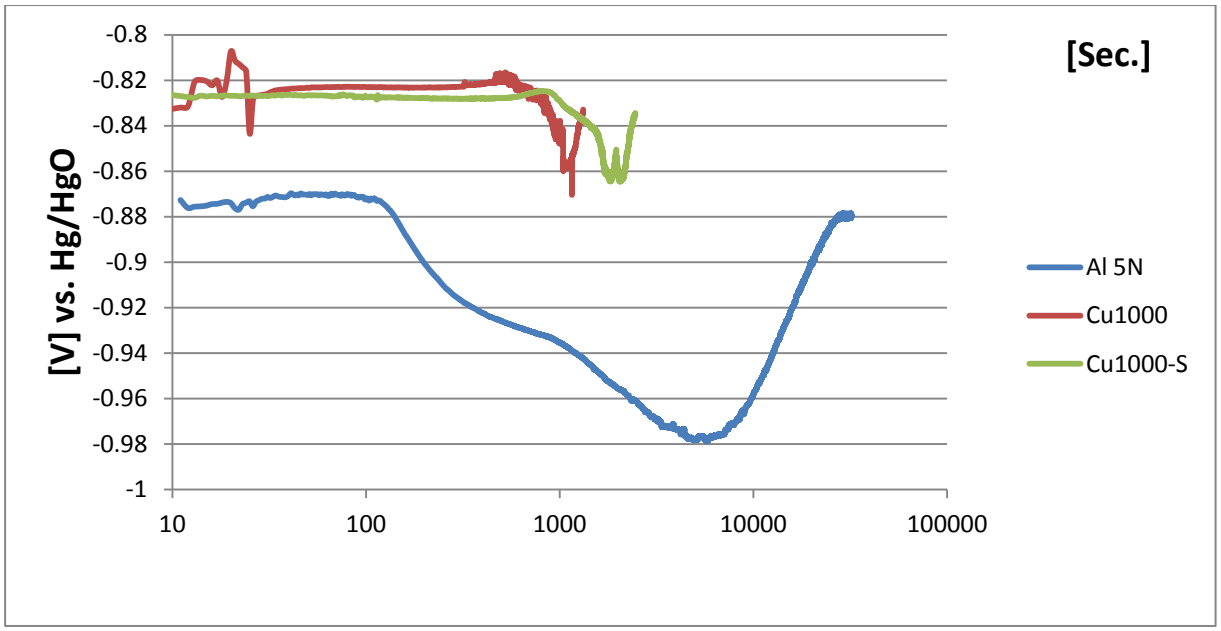

Figure 4.3.4.a: Graph showing the corrosion potential results from pure aluminum and AlCu1000 at 25°C. The difference between Cu1000 and Cu1000-S is that the Cu1000-S has been lowered into the etching bath so that the paint line is equal to the surface of the HCl bath.

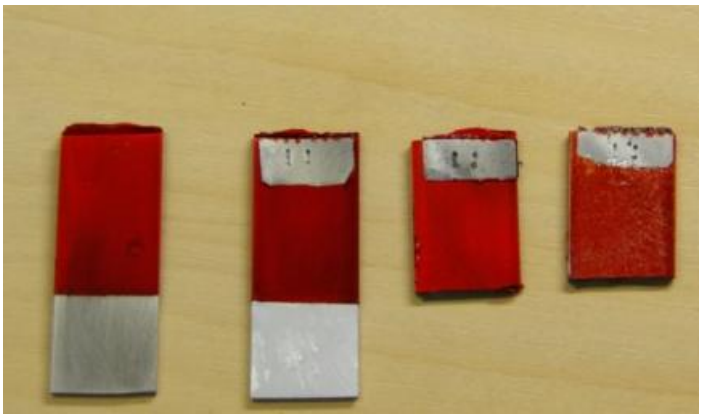

Figure 4.3.4.b: Picture showing test specimens before and after being used in corrosion potential tested. Left specimen shows how all the specimens looked before the corrosion potential test. Second specimen from the left shows the pure aluminum after being tested. The two specimens to the right show how the AlCu1000 specimens looked after the tests.

4.4 Intergranular Corrosion (IGC)

After a special heat treatment of the alloys containing copper, signs of Intergranular Corrosion (IGC) were looked for on the surface. When investigating the test specimen in light microscope and IFM microscope only small indications of a higher etching rate on the grain boundaries could be detected in a few points in the AlCu1000-alloy. By measuring the height difference between the grains and the center of the grain boundary, it could be seen that the grain boundaries had etched between 1.5-3µm more than the grains in certain points. Figure 4.4 shows a picture of a grain boundary that has been etched slightly more than the grains. This preferential etching of the grain boundary is not enough to decide if there are traces of IGC in the alloy, further investigations on grain boundaries inside the test specimen have to be done to conclude if the alloy is exposed to this problem. Due to the low etching rate on the grain boundaries and because only a few boundaries showed preferential etching, no further investigation was done to see if the alloy was exposed to IGC. No preferential etching of the grain boundaries was detected on alloy containing less than 1000 ppm copper.

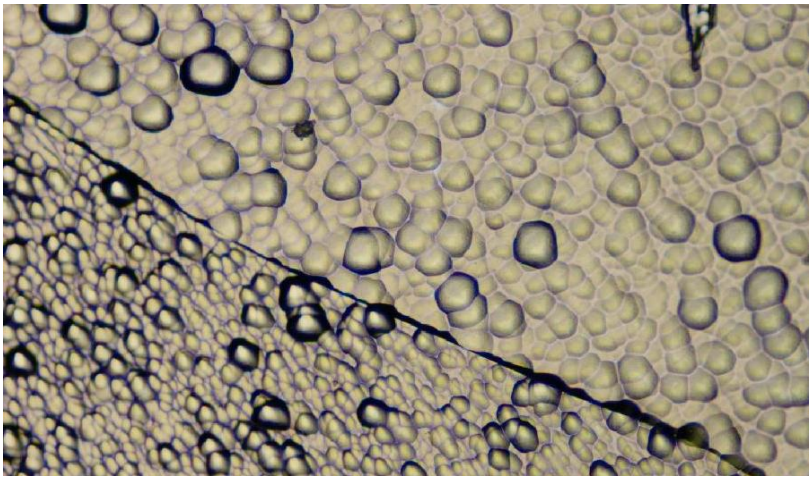

Figure 4.4: Picture showing a grain boundary on an AlCu1000-alloy that shows a slightly higher (1.5-3 µm) etching depth compared to the grains.

CHAPTER 5

Discussion

5.1 Effect of copper on the etching morphology

The difference in etching rate between grains having different crystallographic orientations could be seen and measured in some points on the surface of alkaline etched pure aluminum. From EBSD investigations it could be detected that grains close to the [111] crystallographic orientation showed a higher etching rate than grains having other orientations. By alloying aluminum with copper an even higher etching rate could be measured for grains having this crystallographic orientation. This observation together with the drastically higher weight loss from aluminum-copper (AlCu) alloys, and observations showing higher hydrogen development on certain areas on the test specimen during etching, indicates that copper increases the etching rate of all crystallographic orientations, but mostly the [111] oriented grains. Roughness measurements done on pure aluminum shows a lower roughness on grains that have been highly etched in NaOH, while copper alloyed aluminum shows a higher roughness on the highly etched grains something that indicates that copper increases the attack on [111] oriented grains. The increased surface roughness on grains close to the [111] orientation in the AlCu1000-alloy might be due to preferential etching between the aluminum matrix and the copper. From GD-OES measurements done on alkaline etched AlCu1000 an increasing amount of copper was discovered close to the etched surface, inside the oxide layer. This might be due to dissolution of the less noble aluminum or depletion/diffusion of copper to the surface causing an enrichment of copper that again produces pitting types of corrosion attacks that again increases the roughness of the surface. From corrosion potential tests done on AlCu1000-alloys it is possible to see that the corrosion potential increases as the time goes indicating from [10] that the transition from (a) to (b)in figure 2.3.a increases the dissolution rate of the less noble aluminum causing small pits on the surface around the copper enriched areas that causing a higher roughness.

When etching the same pure aluminum and AlCu-alloys in an acidic environment little or no etching happened for the first few hours. After about 5 hours a black layer started to form on the surface of the AlCu1000-alloy. Normally 65% nitric acid or Chrome Phosphoric acid is used to remove smut layers that is produced on the surface of etched aluminum alloys, since these two acids does not etch aluminum. But after trying both 65% nitric acid at 25^{o}C and Chrome Phosphoric acid at 90^{o}C nothing happened to the surface layer. This result compared with the EDS results showing large amounts of

aluminum and low amounts of copper, indicates that the layer is existing mainly of aluminum. Further it can also be discussed if the porous surface has formed because depleted/diffused copper on the surface has been working as cathodes causing the aluminum matrix around the copper particles to corrode so that the copper eventually falls off, leaving a porous aluminum surface. By removing the surface layer lowering the test specimen into 1.25 molar NaOH solution at 25°C for 1 minute a few micrometers of the layer was removed and the grain structure was easier to examine. From earlier research investigated in the theory chapter it was found that the [001] grains etched more in HCl acid. But after etching away the surface layer using NaOH no signs of this could be detected at the AlCu1000 surface.

5.2 Mechanism of grainy appearance

Since a higher grade of preferential etching was found in AlCu-alloys containing high amounts of copper and GD-OES investigations showed that copper enriches close to the surface during alkaline etching. It is likely that the copper enriches on the surface before it dissolves into the etching bath during etching, and that no crystallographic orientations traps more copper on the surface than others since EDS results from highly etched grains showed the same results as less etched grains.

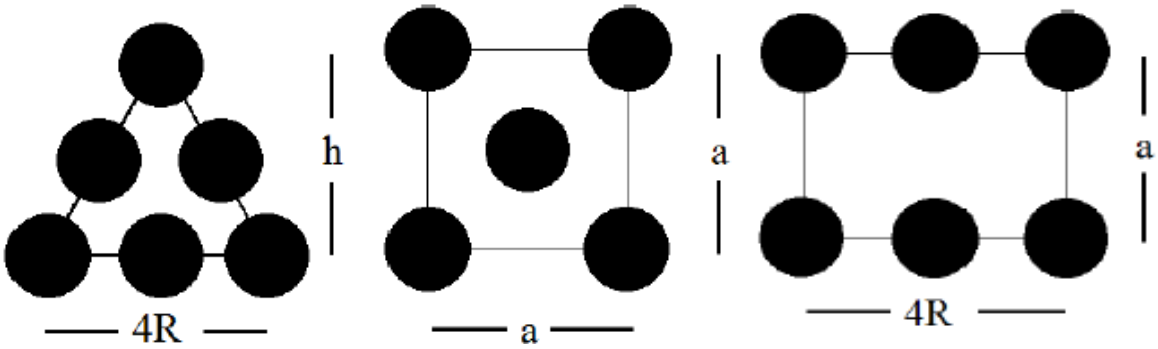

Figure 5.2: Left picture showing the surface area of the [111] plane. Middle picture shows the surface area of the [100] plane. Right picture shows the surface are on the [110] plane. {28}

Probable mechanisms for the higher etching rate of grains having a crystallographic orientation close to the [111] orientation might be due to the higher packing factor shown in table 5.2 of the [111] orientation and the higher surface energy appearing along this plane, causing a tribocorrosion effect that increases the corrosion. Table 5.2 shows the packing factors of the planes occurring in the three different planes in the aluminum FCC structure.

Plane	Packing factor
[111]	0.91
[110]	0.56
[100]	0.79

Table 5.2: Table showing the packing factor calculated in appendix A for the three crystallographic planes in the aluminum FCC structure.

5.2 Future work

As a result of the work done in this master project, the following subjects are suggested for further work:

- Further etching experiments in NaOH solution in order to support the difference in etching rate and roughness between grains showing different crystallographic orientations should be made.
- Alkaline etching of AlCu-alloys containing more than 1000 ppm copper should also be investigated to see if any intergranular corrosion or other types of corrosion can be detected.
- A new method for corrosion potential tests at higher temperatures should be made so that it can be possible to measure the corrosion potential over a longer period of time.
- A closer look at the etching of grains taking the rolling direction of the test material into consideration should be done to see if this affects the etching of grains having different crystallographic orientations.
- Weight loss experiments using different concentrations of HCl to see if it is possible to get a better etching result without creating the surface layer that was formed on AlCu1000-alloys in this project. The surface layer makes it hard to see if a higher etching rate of the [100] crystallographic orientation actually happens. Another possibility is to use the same 4 molar solution and to abort the experiment when certain areas on the surface show a higher etching rate.
- GD-OES investigations on the surface layer created when etching AlCu1000-alloys in HCl should be done to find the types of elements that occur in the layer. A depth profile of the surface layer and the layer/bulk border would also be interesting to have so that it can be possible to see if there are any Cu built ups under the surface layer.

CHAPTER 6

Conclusions

- An increased weight loss and height differences between grains was observed for aluminum with an increasing amount of copper. This indicates that the copper has a major effect on the preferential etching of AlCu-alloys. This together with the GD-OES results that shows an increasing amount of copper close to the surface of the NaOH etched test specimens indicates that the etching increased over time due to an increasing amount of copper close to the surface.
- Preferential etching of grains in AlCu-alloys is most likely occurring due to a galvanic effect between the copper and the aluminum in combination with the higher surface energy of the [111] oriented grains.
- By increasing the copper content in the aluminum an increase in the corrosion potential could be detected for the alkaline etched specimens. This together with the GD-OES results that shows an increasing amount of copper on the surface indicates that the copper content close to the surface changes the corrosion potential of the alloy
- Roughness measurements done on the alkaline etched alloys showed that grains close to the [111] orientation in the pure aluminum showed a lower roughness than grains close to the same orientation in the AlCu1000 alkaline etched specimens indicating that copper increases the roughness of highly etched grains.
- GD-OES measurements done on AlCu1000 has shown that copper enriches close to the surface of the oxide layer and in some cases desmutting the specimen in 65% nitric acid after etching removed some of the copper close to the surface. This indicates that the nitric acid removes small amounts of loosely bounded copper from the surface.
- From HCl etching experiments done on pure aluminum and AlCu1000-alloys no difference in the etching of the crystallographic orientations could be detected against the NaOH etched alloys. The biggest difference between etchings in HCl compared to NaOH was seen on the surface of the AlCu1000-alloy that had developed a black/grey porous surface layer that was firmly bounded to the bulk surface.

References

1. *WERNICH, R. PINNER and P. G. SHEASBY, Surface treatment and finishing of aluminum and its alloys, fifth edition, , volume 1, page 196-197*
2. *WERNICH, R. PINNER and P. G. SHEASBY, Surface treatment and finishing of aluminum and its alloys, fifth edition, volume 1, page 196-197*
3. B.Holme, N. Ljones, A. Bakken, O Lunder, J. E. Lein, L. Vines, T. Hauge, Ø. Bauger, and K. Nisancioglu, Preferential Grain Etching of AlMgSi (Zn) Model Alloy, Journal of The Electrochemical Society, 157 (12) C424-C427, 2010, page 1
4. B.Holme, N. Ljones, A. Bakken, O Lunder, J. E. Lein, L. Vines, T. Hauge, Ø. Bauger, and K. Nisancioglu, Preferential Grain Etching of AlMgSi (Zn) Model Alloy, Journal of The Electrochemical Society, 157 (12) C424-C427, 2010, p. 2-3
5. N. Jones, Grainy appearance on anodized profiles, Master's thesis, 2006, p. 40
6. E.V. Koroleva, G.E. Thompson, P. Skeldon, and B. Noble, *Proc. R. Soc. London, Ser. A,* **436,** 1792 (2007)
7. B.Holme, N. Ljones, A. Bakken, O Lunder, J. E. Lein, L. Vines, T. Hauge, Ø. Bauger, and K. Nisancioglu, Preferential Grain Etching of AlMgSi (Zn) Model Alloy, Journal of The Electrochemical Society, 157 (12) C424-C427, 2010, page 1
8. S.Wernic, R. Pinner, and P.G. Sheasby, The Surface Treatment and Finishing of Aluminum and its Alloys, Volume 1, fifth edition
9. Yoshimasa Takayama, Kentaro Nohara, and Hajime Kato, Influence of Crystallographic Orientation on Corrosion Behaveor of 5N Purity Aluminum, Proceeding of the 12th International Conference on Aluminum Alloys, 2010
10. H.W pickering, Department of Materials Science and engineering, The Pennsylvanian State University, Corrosion Science Vol. 23, No10, Characteristic Features of Alloy Polarization Curves, 1983
11. N. Dimitrov, J.A. Mann, and K. Sieradzki, Journal of The Electrochemical Society, 146, Copper Redistribution during Corrosion of Aluminum Alloys
12. D.Y. Jung, I. Dumler, and M. Metzger, Electrochemical Science and Technology, Electronmicroscopic Examination of Corroded Aluminum-Copper Alloy Foils, 1985
13. S. Garcia-Vergara, F. Collin, P. Skeldon, G.E. Thompson, P. Bailey, T. C. Q. Noakes, H. Habazaki, and K. Shimizu, Journal of The Electrochemical Society, 151, Effect of Copper Enrichment on the Electochemical Potential of Binary Al-Cu Alloys, 2004
14. S.Wernick, R. Pinner, and P.G. Sheasby, The Surface Treatment and Finishing of Aluminum and its Alloys, Volume 1, Fifth edition.
15. Magnus Hurlen Larsen, John Charles Walmsley, Otto Lunder, Ragnvald H. Mathiesen, and Kemal Nisancioglu, Intergranular Corrosion Of Copper Containing AA6xxx AlMgSi Aluminum Alloys, Journal of The Electrochemical Society, 155 (11) C550-C556 (2008)].
16. Magnus Hurlen Larsen, John Charles Qalmsley, Otto Lunder, and Kemal Nisancioglu, Effect of Excess Silicon and Small Copper Content on Intergranular Corrosion of 6000-Series Aluminum Alloys, Journal of The Electrochemical Society, 157 (2) C61-C68 (2010) p 1-2
17. G. Svenningsen, J.E. Lein, A. Bjørgum, J.H. Nordlien, Y. Yu, and K. Nisancioglu, *Corr. Sci.,* 48, 226 (2006) – G. Svenningsen, M.H. Larsen, J.C. Walmsley, J.H. Nordlien, and K. Nisancioglu, *Corros. Sci.,* 48, 1528 (2006) - G. Svenningsen, M.H. Larsen, J.C. Walmsley, J.H. Nordlien, and K. Nisancioglu, *Corros. Sci.,* 48, 258 (2006) - G. Svenningsen, M.H. Larsen, J.C. Walmsley, J.H. Nordlien, and K. Nisancioglu, *Corros. Sci.,* 48, 3969 (2006)

18. F. King, Ellis Horwood Series in Metals and Associated Materials, Aluminum and its Alloys, 1987
19. F. King, Aluminum and its alloys, 1987, page 177
20. F. King, Aluminum and its alloys, page 92
21. J.R Davis, Davis & Association, The material Information Society, Aluminum and Aluminum Alloys, Second printing, page 291
22. Teknologiske metaller og legeringer, Professor Jan Ketil Solberg, Institutt for materialtekonologi, NTNU, 2007, page 201
23. J.R Davis, Davis & Association, The material Information Society, Aluminum and Aluminum Alloys, Second printing, page 291
24. Scanning electron microscopy, J. Hjelan, 1989
25. Nina Ljones, Grainy appearance on Anodized Profiles, 2006
26. Lecture notes in Tribology and Surface Treatmen, TMM 4205 Elastohydrodynamic Lubrication, 2011
27. Jan Ketil Silberg, Lysmikroskopi, 1998.

List of figures

List of tables

Appendix A

Packing factors of planes

The Face Centered Cubic (FCC) cell is shown in figure A1 has a packing factor of 0.76.

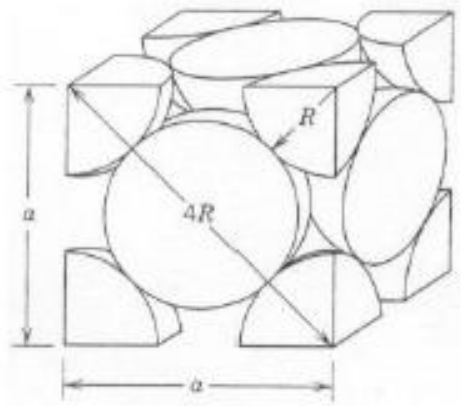

Figure A1: Picture shows how the FCC cell is constructed.

$$a^2 + a^2 = (4R)^2$$

Solving for a:

$$a = 2R\sqrt{2}$$

The atomic packing factor of the [111] plane:

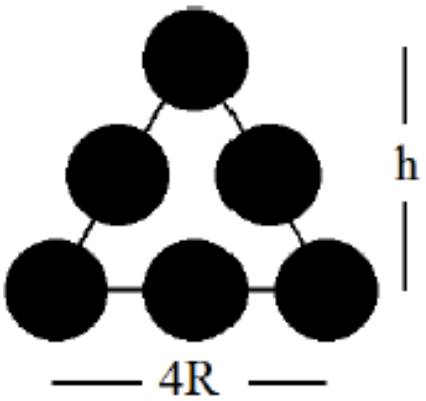

Figure A2: Surface area of the [111] plane

$$(\frac{1}{2} * 4R)^2 + h^2 = (4R)^2$$

Solving for h:

$$h = 2\sqrt{3}R$$

The total surface area of the [111] plane is:

$$A_{[111]} = \frac{1}{2} * 4R * 2\sqrt{3}R = 4\sqrt{3}R^2$$

Using the total area of two atoms in the [111] plane, the atomic packing factor can be calculated:

$$APF = \frac{2\pi R^2}{4\sqrt{3}R^2} \cong 0.91$$

The atomic packing factor of the [001] plane:

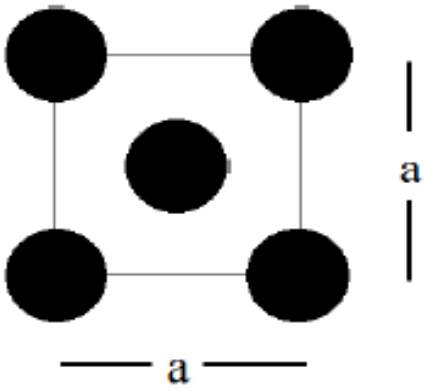

Figure A3: The surface are of the [001] plane

The total surface area of the [001] plane:

$$A_{[001]} = a^2 = (2R\sqrt{2})^2 = 8R^2$$

With a total area of two atoms in the [001] plane, the atomic packing factor can be calculated:

$$APF_{[001]} = \frac{2\pi R^2}{8R^2} \cong 0.79$$

The atomic packing factor of the [110] plane:

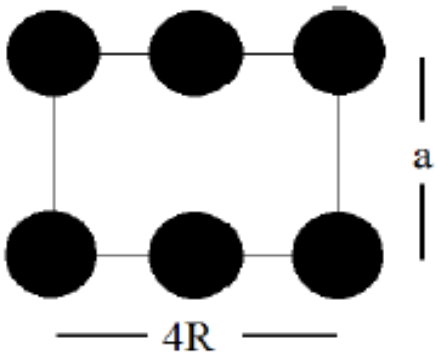

Figure A4: The surface area of the [110] plane

The total surface area of the [110] plane:

$$A_{[110]} = a * 4R = 2R\sqrt{2} * 4R = 8\sqrt{2}R^2$$

With a total area of two atoms in the [110] plane, the atomic packing factor can be calculated:

$$APF_{[110]} = \frac{2\pi R^2}{8\sqrt{2}R^2} \cong 0.56$$

Appendix B

Rq and Ra calculations:

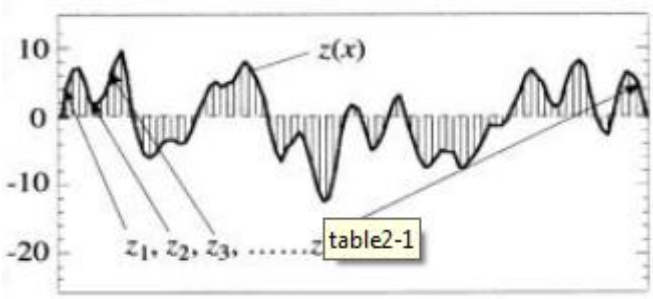

Figure A5: Graph showing roughness measurements. L equals to the length of the measurements and is showed on the x-axis.

$$R_a = \frac{1}{L}\int_0^L |z(x)|dx$$

$$R_a = \frac{\sum|z(x)|}{n}$$

The R_a value is the average distance from the profile's center line. This is the most used value in the industry. The R_a value gives limited information about the surface topography.

$$R_q = \sqrt{\frac{1}{L}\int_0^L z(x)^2 dx}$$

The R_q (root mean square) value is a better characterization of the profile since the highest peaks and lowest valleys influence the value more than for the R_a {26}.

Appendix C

Settings used in EBSD

NORDIF:

Software version:	1.4.0

Microscope:

Manufacturer:	Zeiss
Model:	Ultra 55
Magnification:	152-160
Accelerating voltage:	20.0kV
Working distance:	20mm
Tilt angle:	70.0°

Signal voltages:

Minimum:	-1.5V
Maximum:	3.5V

Deflection voltages:

Minimum:	-7.8V
Maximum:	7.8V

Electron image:

Frame rate:	0.10fps
Resolution:	800x800px, 1000x1000px
Calibration factor:	5515.1µm/V

EBSD detector:

Model	UF-1000

Appendix D

Parameters used in GD-OES measurements

GD-OES instrument: Horiba Jobin Yvon in radio frequency mode.

Intensity measured every 0.01s.

Sputter rate, metal:	0.07µm/s.
Sputter rate, oxide:	0.04µm/s.
Area analyzed for each test:	0.12 cm^2.
Flushing time:	120 s.
Preintegration time:	70 s.
Background:	5s.
Measurement time:	10 s.
Pressure:	600 Pa.
Power:	32 W.
Module:	7 V.
Phase:	4 V.

GD-OES graphs produced from quantitative data found in AlCu10-alloy.

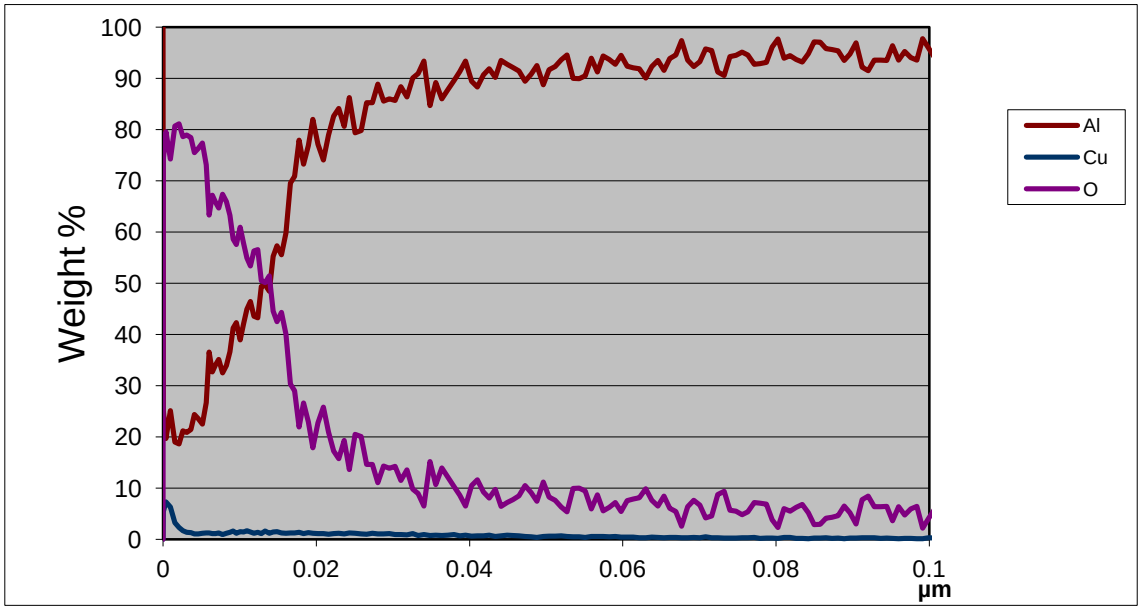

Figure A6:Alcu10-alloy etched at 25°C, not desmutted. Cu graph multiplied by 10.

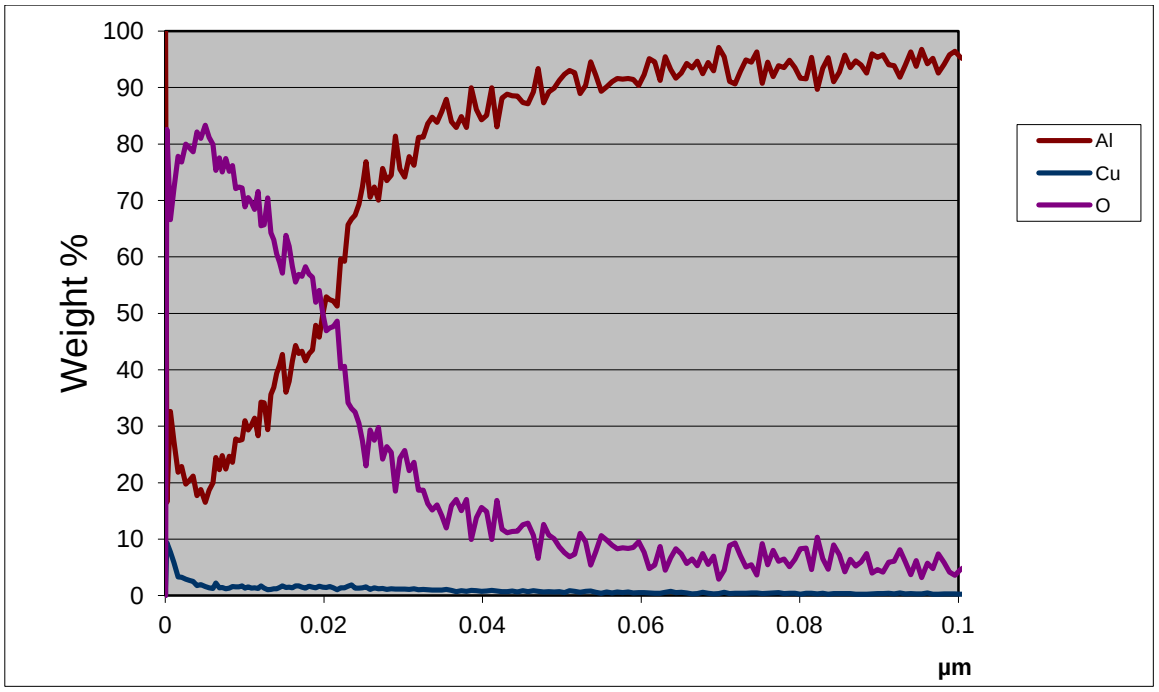

Figure A7: Desmutted AlCu10 sample etched at 25°C. Cu graph multiplied by 10.

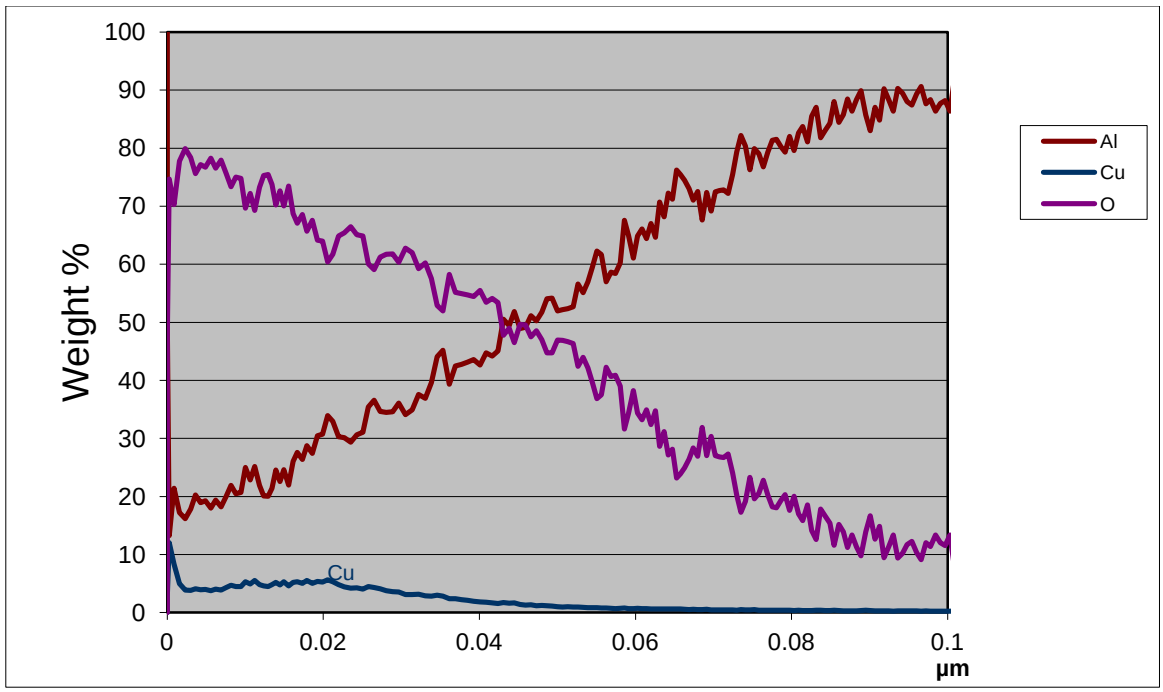

Figure A8: AlCu10-alloy etched at 70°C, not desmutted.

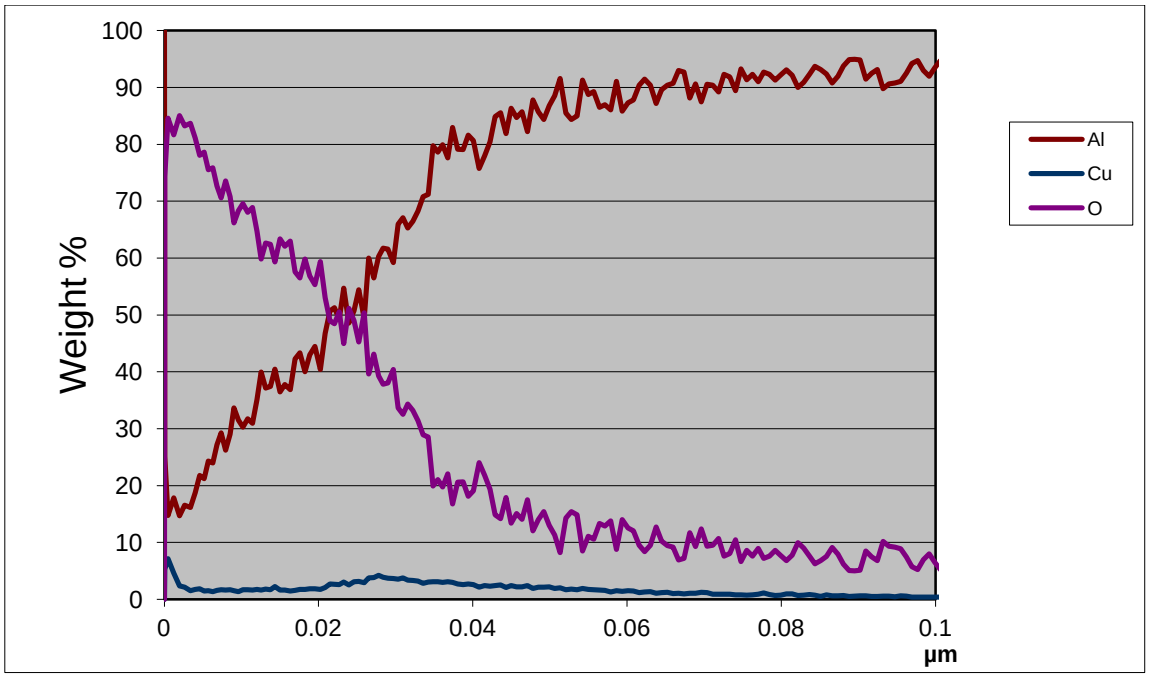

Figure A9: Desmutted AlCu10-alloy etched at 70°C. Cu graph multiplied by 10.